1961

Installation and tests of General Electric Model 5GDY34C1 axial flow fan-dynamometer set

Farber, Karl H.

Monterey, California: U.S. Naval Postgraduate School

INSTALLATION AND TESTS OF GENERAL ELECTRIC MODEL 5GDY34C1 AXIAL FLOW FAN-DYNAMOMETER SET

KARL H. FARBER

INSTALLATION AND TEST OF GENERAL ELECTRIC MODEL 5GDY34C1 AXIAL FLOW FAN-DYNAMOMETER SET

* * * * *

Karl H. Farber

INSTALLATION AND TESTS OF

GENERAL ELECTRIC MODEL 5GDY34C1

AXIAL FLOW FAN-DYNAMOMETER SET

by

Karl H. Farber

Lieutenant, United States Navy

Submitted in partial fulfillment of
the requirements for the degree of

MASTER OF SCIENCE
IN
MECHANICAL ENGINEERING

United States Naval Postgraduate School
Monterey, California

1 9 6 1

NPS Archive
1961
Farber, K

INSTALLATION AND TESTS OF GENERAL ELECTRIC MODEL 5GDY34C1 AXIAL FLOW FAN-DYNAMOMETER SET

by

Karl H. Farber

This work is accepted as fulfilling
the thesis requirements for the degree of
MASTER OF SCIENCE
IN
MECHANICAL ENGINEERING
from the

United States Naval Postgraduate School

ACKNOWLEDGEMENTS

The writer wishes to express his appreciation for the assistance and encouragement given him by Professors Charles P. Howard and Paul F. Pucci throughout the performance of this work. He also wishes to thank Lieutenant James A. Bridge, Jr., U. S. Navy who gave generously of his own valuable time to assist in much of the heavier labor involved in the project and in the operation of the equipment during several of the earliest performance runs.

ABSTRACT

The General Electric Model 5GDY34C1 axial flow fan-dynamometer set was purchased by the Department of Mechanical Engineering of the U. S. Naval Postgraduate School to be used in laboratory instruction of students at the school. The objectives of this thesis were the design, construction, installation, instrumentation and testing of the various components making up the completed installation, and the determination of the performance characteristics of the fan-dynomometer set. These objectives have been met. Although those performance characteristics were determined that could be compared with the typical characteristics provided by the manufacturer, they by no means represent the limit obtainable. Since there are many variations of operating conditions possible for the set, the number of different characteristics possible are virtually unlimited.

TABLE OF CONTENTS

LIST OF ILLUSTRATIONS

List of Illustrations

LIST OF SYMBOLS

Arabic Letters	Description
V	Air velocity
p	Pressure
g	Acceleration due to gravity
Q	Volume flow rate
A	Area
W	Relative velocity vector; dynamometer force
U	Peripheral velocity vector
w	Mass flow rate
C	Nozzle discharge coefficient
F	Velocity of approach factor
d	Nozzle throat diameter in inches
F_a	Nozzle thermal expansion factor
Y_a	Adiabatic expansion factor
h	Differential pressure head
K	Constant
n	Fan speed
t	Temperature
T	Absolute temperature
HP	Horsepower
L	Dynamometer torque arm = 1.31 feet

LIST OF SYMBOLS

Greek Letters	Description
ρ	Density
η	Efficiency
ω	Angular velocity
Subscripts	
v	Velocity
c	Constant
a	Axial when applied to velocity, atmospheric when applied to pressure and temperature
u	Peripheral component
(20°)	Pertaining to blade angle of 20 degrees
H	Hourly rate
w	Pertaining to inches of water when applied to pressure, wet-bulb when applied to temperature
s	Specified when applied to n and ρ , static when applied to p and η
x	Test
p	Partial vapor
g	Saturated vapor

1. Introduction

The General Electric Model 5GDY34C1 axial flow fan-dynamometer set offers students the opportunity to obtain demonstrations of the principles of axial flow fans and compressors. By varying blade angles and stage combinations as well as speed it is possible to illustrate the effect of optimum and off-design operating conditions on the performance of these types of machines.

The objectives of this thesis were to complete the installation of the test set-up and to test the machine to obtain a record of its performance under varying operating conditions. Illustrated in this work are the effects of varying rotor blade angles, stator blade angles, number of stages and fan speed. Also shown are comparisons of the characteristics of the machine operating as both a tube-axial and a vane-axial fan.

2. The Fan-Dynamometer Set.

The Model 5GDY34C1 axial flow fan-dynamometer set was built by the Locomotive and Car Equipment Department of the General Electric Corporation at Erie, Pennsylvania. It was intended to be a piece of comprehensive equipment for college mechanical and aeronautical engineering laboratories.

The unit consists of an axial-flow fan mounted on a common bedplate with a 7-1/2 HP d.c. cradled dynamometer. See Figure 1, page 3. The maximum speed rating of the fan is 3000 RPM, and that of the dynamometer is 3600 RPM. A field rheostat limits the dynamometer speed to the fan rating. Because of inadequate ventilation at lower speeds, the minimum speed of the dynamometer is limited to approximately 500 RPM.

Each stage of the fan contains 24 rotor blades and 37 stator blades. All rotor blades are identical as are the stator blades. Provision is made for rotating both the rotor blades and the stator blades to various angular positions. Two protractor-type templates are provided to assist in adjusting blade angles. The rotor blade is an RAF #6 propellor section with a thickness to length ratio of 12 per cent. The blade has a 4 degree twist from root to tip. Rotor blades are cast individually of an aluminum alloy and used in the "as-cast" state except at the tip where they are machined to maintain a nominal 0.015 inch running clearance. Stator blades, which are made of sheet steel, are shaped in the form of a circular arc, and have 8 degrees of twist from root to tip.

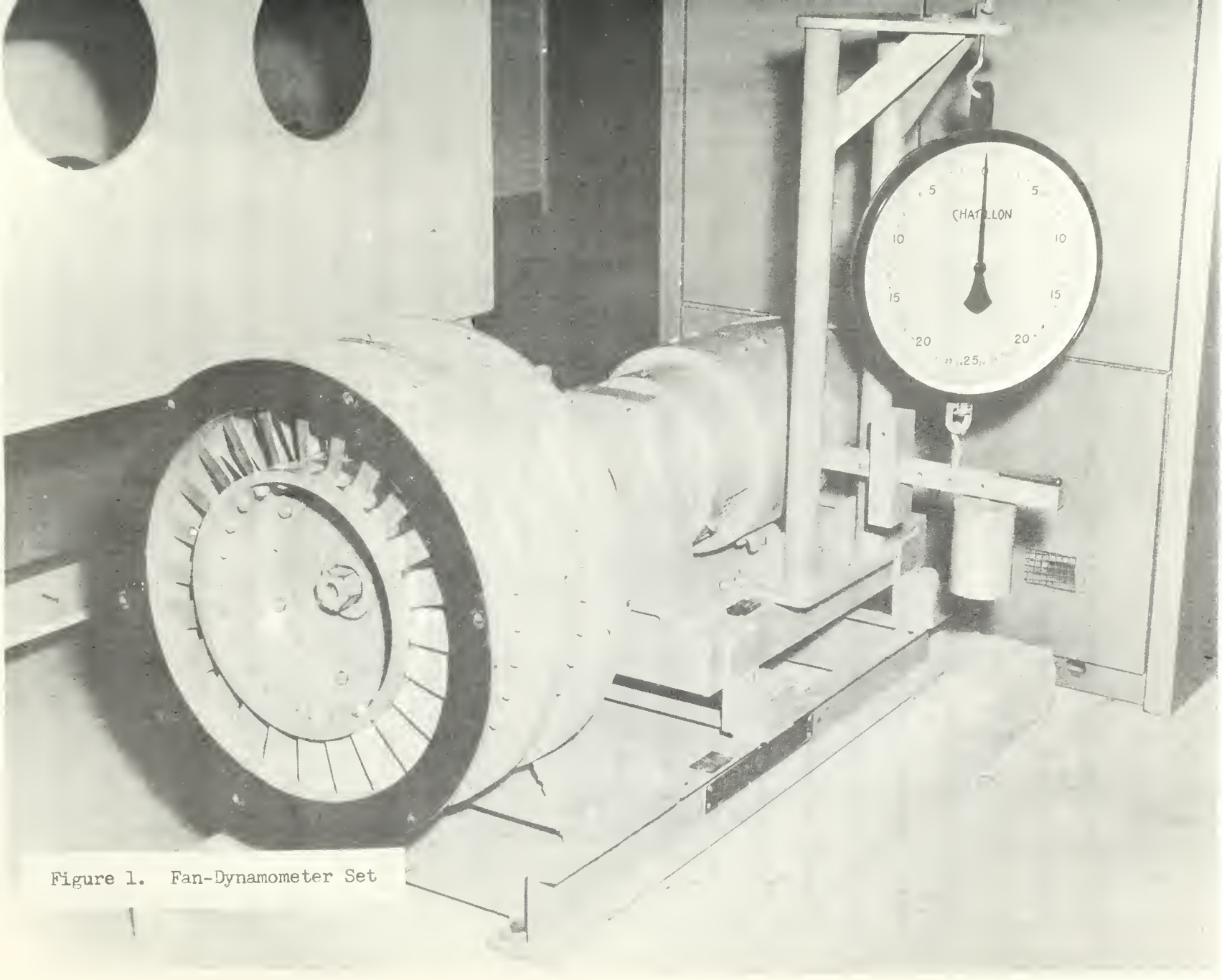

Figure 1. Fan-Dynamometer Set

The fan consists of two stages. The first stage stator mounts on the pedestal-supported flange. The first stage rotor mounts on the front-shaft extension and is held by a lock-nut. The second stage stator flange-mounts to the first stage stator, and likewise, the second stage rotor flange-mounts to the first stage rotor. The fan may be disassembled from the front without exposing the bearings and without disturbing alignment. One "blank" first stage stator, one "blank" second stage stator, and one "blank" second stage rotor are available. None of these is equipped with blades. They may be used in substitution for a particular stage when desired. Also available are one spare each of first and second stage stators and two spare rotors. These pieces are equipped with blading and allow the adjustment of blade angles of the stages for a particular laboratory setup at the same time that the equipment is being used with a different setup.

Reference [1]* describes in detail the method of adjusting blade angles. The manufacturer prescribes the use of a torque wrench in tightening the lock nuts on the blades after they have been adjusted, and cautions against exceeding a torque of 4 to 5 pound-feet on the rotor blades and 8 to 10 pound-feet on the stator blades. However, the rotor blades in the machine as received from the manufacturer were found to be torqued to values exceeding 10 pound-feet, and indeed, it was found necessary to tighten the lock nuts to about 6 pound-feet in order to obtain sufficient clearance between the blades and the housing at operating speed. Caution must be used in tightening the lock nuts to ensure that the torque applied is sufficient to overcome the friction in the

*Numbers in brackets pertain to references listed in Bibliography, page 40.

threads. At such low values of torque it is a simple matter to leave the blades in an unsecured condition if the torque applied is not enough to overcome thread friction.

Scribe marks were placed on the protractors corresponding to the blade angles most commonly used. It was found that this action was necessary in order to save a great deal of time in adjusting the blade angles, since it is extremely easy to disturb the protractor setting even though a locking set screw is provided to prevent this.

Disassembly and reassembly of the stators and rotors can be accomplished by one person. However, the stators are quite heavy, and the assistance of a second person or a hoist in handling them is to be recommended. Care must be exercised in handling these parts to prevent damage to the blades.

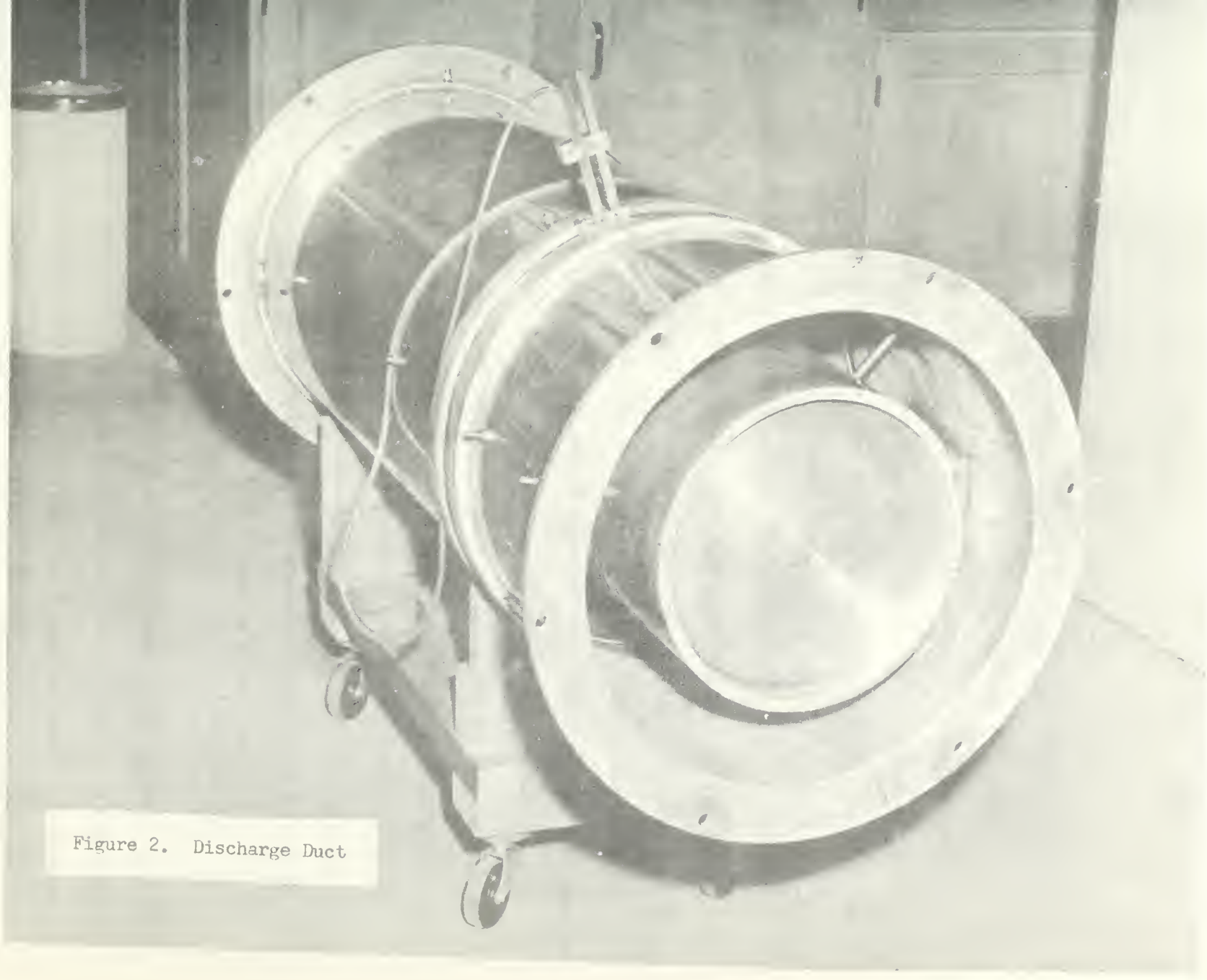

Figure 2. Discharge Duct

3. The Discharge Duct.

An annular discharge duct connects the outlet of the fan to the plenum chamber. See Figure 2, page 6. This duct is four feet in length. The inside diameter of the outside duct is 18 inches and the outside diameter of the inner duct is 12-3/8 inches, corresponding to the dimensions of the fan. The air discharges from the fan through the annulus and into the plenum chamber. The inner duct is blanked off at both ends to prevent leakage of air to the inside.

A rotating slip-ring arrangement has been provided in the outer duct approximately three feet down-stream from the fan. Mounted on the slip-ring is a stand for a total pressure probe. This arrangement allows total pressure surveys to be made across and completely around the annulus. Also, at a location just upstream of the total pressure probe, is a static pressure tap. Connection of this pressure tap to one side of an inclined differential manometer, while the other side is connected to the total pressure probe, allows the measurement of dynamic head in the duct. Another static pressure tap at the entrance to the duct provides for the measurement of the fan discharge static pressure. The inner and outer ducts are separated and maintained in proper relative position by twelve 1/4 inch tie-bolts. These tie-bolts are located at four stations along the length of the duct. At each station are three bolts equally spaced at 120 degree intervals around the circumference of the duct. Inside the annulus, the bolts pass through sleeves which act as spacers to maintain the proper distance between the ducts.

A small dolley is provided for transporting the discharge duct during connection and disconnection.

4. The Plenum Chamber

The plenum chamber into which the air discharges from the duct is cubic in shape, measuring four feet on each side. The walls consist of 3/4 inch plywood supported by a sturdy framework of 2 x 4 s. The top, which is removable to allow access to the plenum chamber, is double-walled, having a 1/4 inch plywood inner wall in addition to the outer wall. In a like manner, the side walls are partially lined with 1/4 inch plywood in a manner and for a reason which will be described shortly.

The air reaching the plenum chamber through the duct described in the previous section discharges through an annular entrance into the chamber. This entrance may be clearly seen in Figure 3, page 9. A throttling mechanism has been provided inside the plenum chamber to allow control of air flow rate from the fan. This mechanism, which is shown in Figure 5, page 11, closes off the annulus through which the air flows into the plenum chamber. The amount of closure is controlled by a handwheel located outside of the chamber. The closure device is a tapered wooden ring which may be advanced into the annulus so as to decrease the flow area.

Situated in the top of the plenum chamber are four flow metering nozzles. Two of these have throat diameters of 3.875 inches while the other two are 9.000 inches in diameter. Caps are provided for closing off nozzles not in use.

Inside the plenum chamber, approximately 10 inches below the nozzles are two layers of horizontally-positioned four-to-the-inch wire mesh screen serving as flow-straighteners. The side walls of the

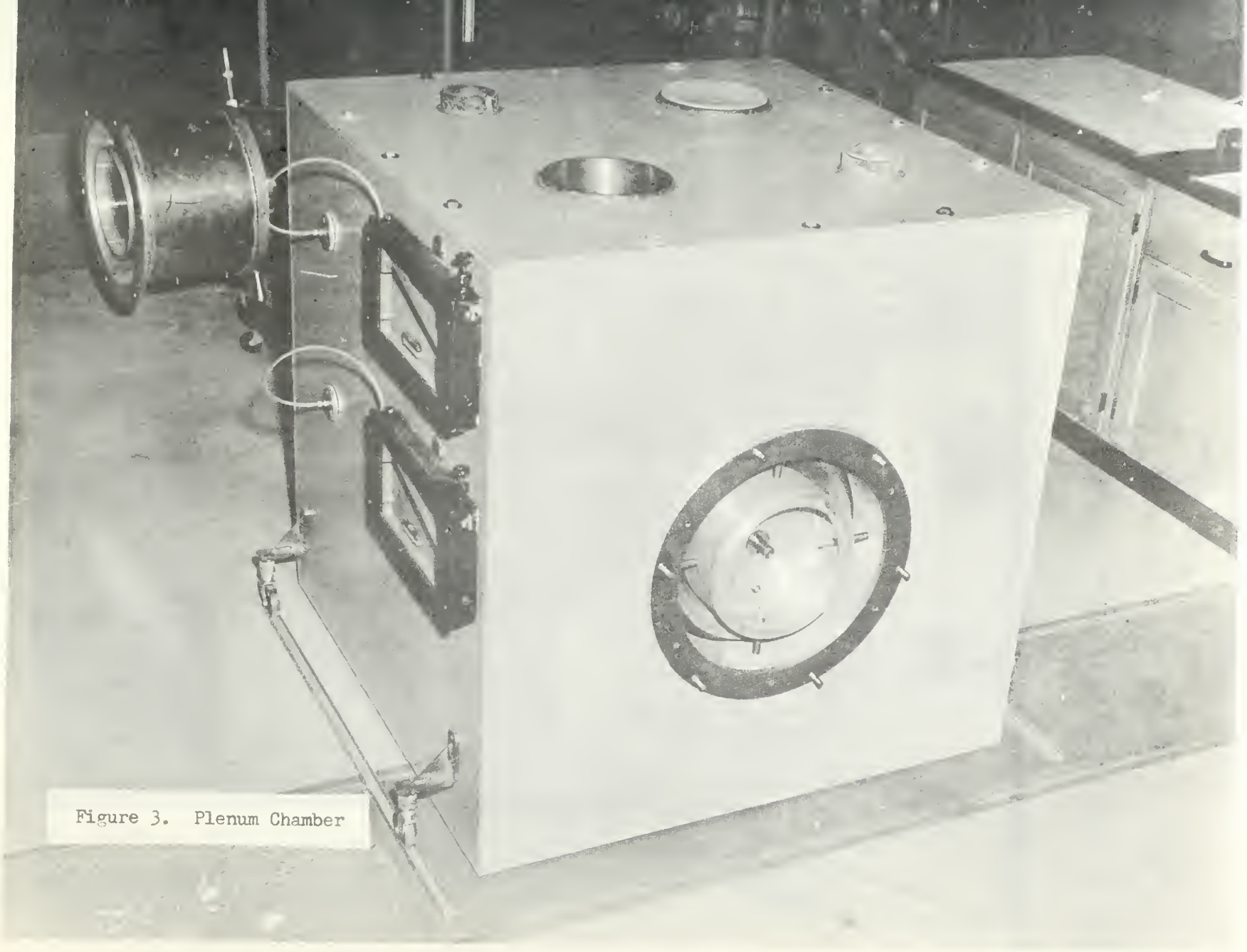

Figure 3. Plenum Chamber

Figure 4. Complete Assembly

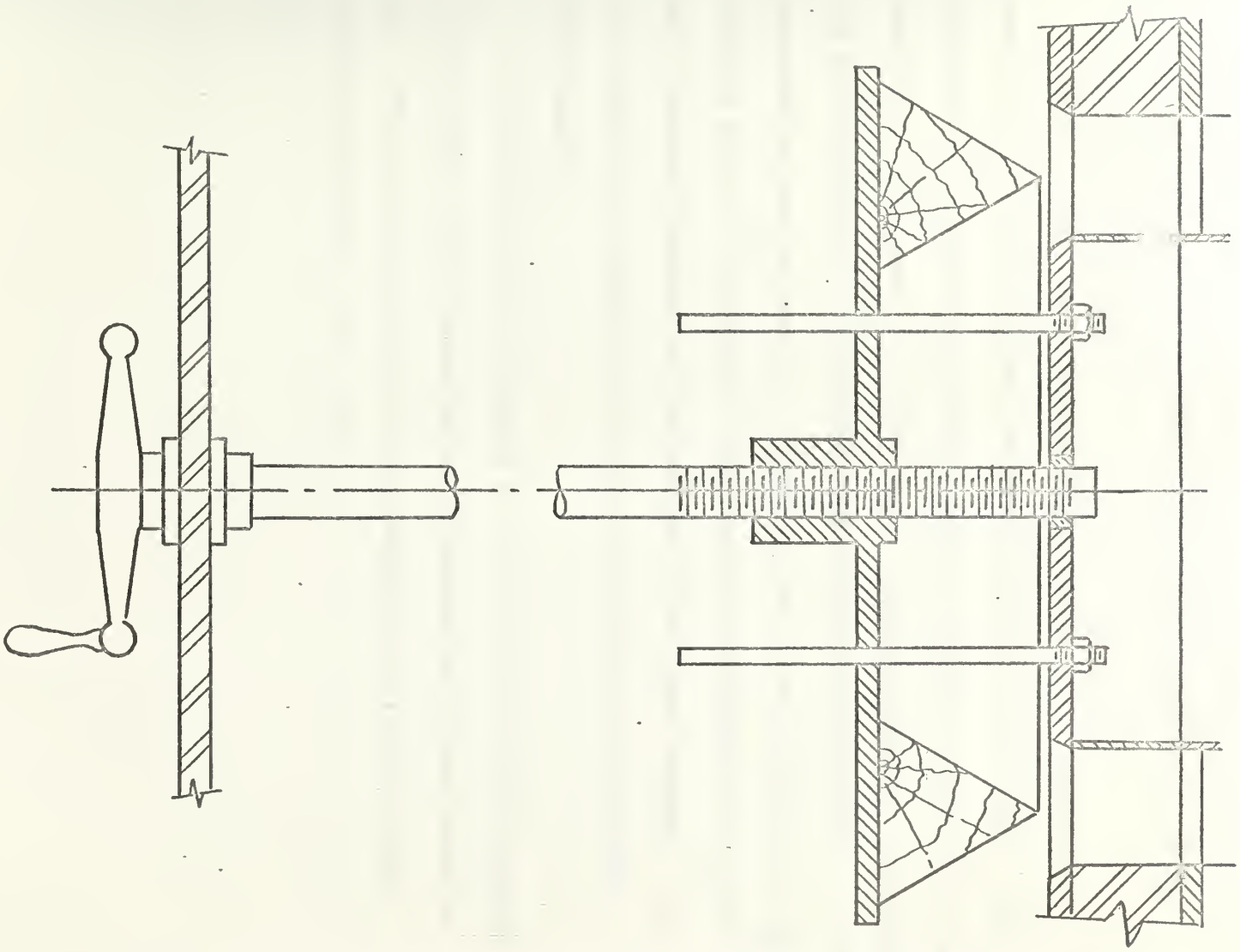

Figure 5. Sketch of flow throttling device. Tapered wooden ring plug advances to the right closing off flow channel.

chamber are lined on the inside above the mesh screens, as mentioned earlier, to maintain uniform flow upward to the nozzles and to retard turbulence at the walls.

There are two static pressure taps in the plenum chamber, one being located below the flow-straighteners and the other above. The uppermost tap provides the static pressure reading at the inlet to the nozzles for determination of flow rate, while the lowermost tap allows the determination of the pressure drop across the straighteners. This pressure drop varied from 0.01 to 0.15 inches of water during the performance tests. In addition to these pressure taps which are connected to manometers mounted on the outside of the plenum chamber, there is a thermometer located in one wall, indicating inlet temperature to the nozzles.

The plenum chamber is mounted on four casters to allow movement of the chamber during connection and disconnection of the discharge duct. These casters ride in rails to maintain consistent and convenient positioning of the chamber.

5. Speed Variator.

A speed variator utilizing variable voltage control provides essentially continuously adjustable speed drive over a wide range. It consists of three basic parts; a d.c. dynamometer as the driving motor, a motor-generator set, and associated control equipment.

Speed adjustment from minimum speed to base speed (2000 RPM at dynamometer rated full load) is provided by means of generator field control. Adjustment from base speed to maximum speed is obtained by dynamometer field control. The generator field rheostat and dynamometer field rheostat are mounted as a unit with a common shaft and control knob. They are connected mechanically so that as their common shaft is turned from one extreme toward the other, the arm of one rheostat remains stationary while the arm of the other rotates. At approximately mid travel of the shaft, their operations reverse so that for the remaining travel of the shaft the arm that was formerly stationary rotates and vice versa. Thus, by turning the rheostat knob from the minimum speed position through the full travel, the dynamometer speed may be adjusted between a minimum and a maximum value.

The speed variator power unit may be seen at the far end of the fan-dynamometer in Figure 1, page 3 and also at the right in Figure 4, page 10.

6. Performance Tests.

Upon completion of the design, construction, installation and instrumentation of the various components of the equipment tests were first made to determine the ability of the set-up to perform its function.

Velocity pressure surveys were conducted at various positions in the traverse plane of the duct using the rotatable slip ring arrangement and the total pressure probe described under the section entitled "Discharge Duct". From these surveys velocity profiles in the flow channel were determined. First, radial velocity profiles were established at four different locations. Three of these locations were situated midway between the supporting struts in the duct and the fourth was directly in the wake of one of the struts. The air velocity was calculated from the equation

$$V = \sqrt{\frac{2 g_c p_v}{\rho}}$$

where V is the air velocity in feet per second, p_v is the velocity pressure in pounds per square foot, g_c is the conversion constant ($32.2\ lb_m\text{-}ft\ /\ lb_f\text{-}sec^2$), and ρ is the air density in pounds per cubic foot. The velocity was then plotted against the radial distance between the walls of the duct. A typical profile of the flow between the struts can be seen in Figure 6a, page 15, and a typical profile of the flow in the wake of a strut is shown in Figure 6b, page 15. These profiles were obtained with a fan speed of 940 RPM and a flow rate of about 1625 CFM.

Following this a survey was taken at the mean radius of the flow channel in a circumferential direction. Pressure readings were converted

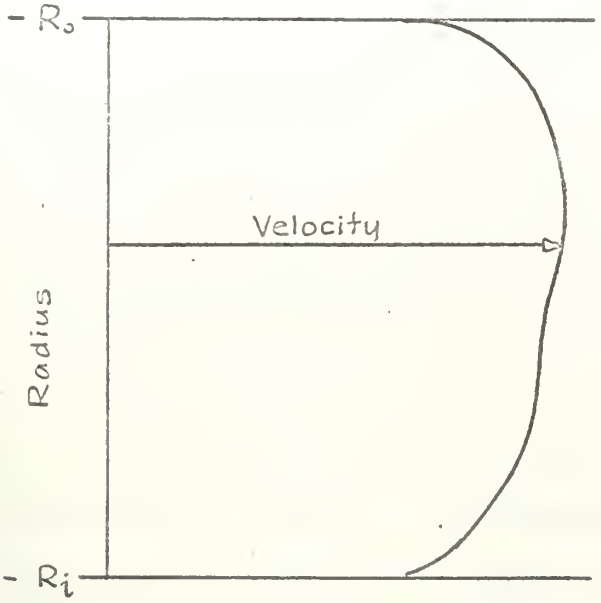

Figure 6a. Radial velocity profile between struts.

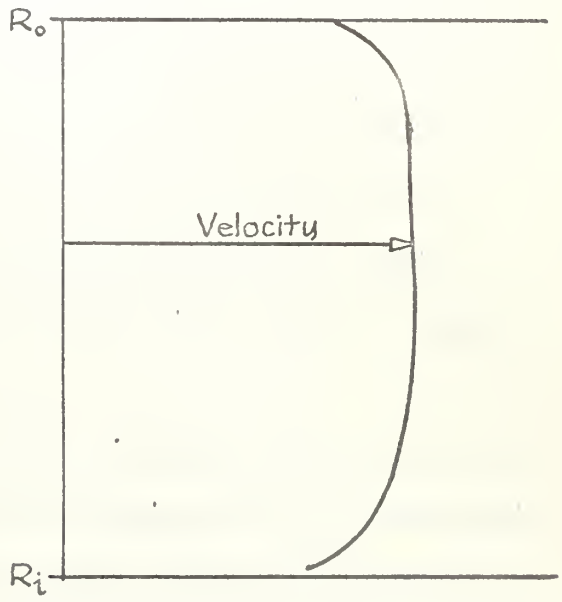

Figure 6b. Radial velocity profile in wake of strut.

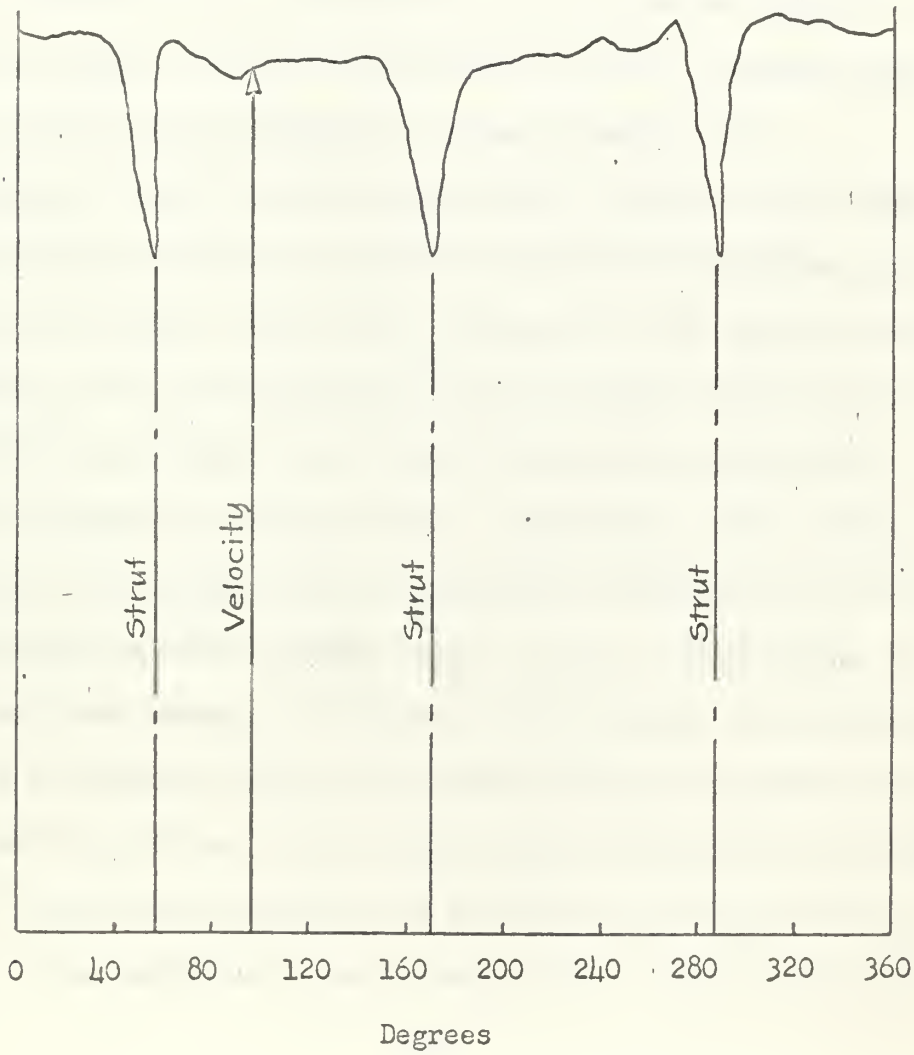

Figure 7. Velocity profile in peripheral direction around annulus taken at mid radius of flow channel.

to velocities in the same manner as described just previously, and velocities were plotted versus angular position around the annulus. The velocity profile in the circumferential direction, also taken at a fan speed of 940 RPM and a flow rate of 1625 CFM, is shown in Figure 7, page 15.

These velocity profiles indicate fairly uniform conditions around and across the annulus. The irregularities existing in the circumferential velocity profile are probably due to minor imperfections in the walls of the duct and to the supporting struts further upstream of the survey area. These are not considered to be of a serious nature. At any rate, the results of these preliminary tests were considered sufficient to establish the suitability of the discharge duct.

Following the tests in the discharge duct, extensive tests were conducted to evaluate the performance of the four flow-metering nozzles. Velocity pressure surveys were conducted at the throats of each of the nozzles. From this information, which yielded a velocity profile for each nozzle throat, the volume flow rate was determined in the manner prescribed in Reference [2] . Essentially, this consists of determining the average velocity existing at the throat and multiplying this by the area of the throat, since $Q = AV$. These values of flow rate were then compared with those values determined by measuring the pressure differential across the nozzles, and assuming that the discharge coefficients for A.S.M.E. "long radius" nozzles were applicable. The results from these two methods are described in greater detail in Appendix A. It is sufficient here to mention that where the A.S.M.E.

discharge coefficients did not apply, the nozzles were calibrated in such a manner as to provide accurate indications of volume flow rate.

At the conclusion of all of these tests it was determined that the equipment was capable of determining the performance characteristics accurately of the fan-dynamometer set. The establishment of these characteristics is, of course, the primary theme of this work.

Tests were begun to accomplish this end, and the data obtained from these tests yielded the results shown in Figures 11 through 21 on pages 28 to 38. Illustrated in these figures are curves demonstrating the variation of three basic quantities; namely static discharge pressure, static efficiency and horsepower input with variation of volume flow rate. Many methods of showing performance have been and are still used by different individuals. According to Reference [4], however, the graph constitutes the best way of expressing performance and is most generally used.

As is apparent from the curves, the fan characteristics vary markedly with changes in blade angles and stage combinations. The curves for these various configurations are identified in the following manner. Each curve is labeled with a certain blade angle-arrangement designation except those in Figures 20 and 21, pages 37 and 38, which are labeled according to fan speed. In these designations angles of stator and rotor blades are listed in that order. For example, the designation 64-30 referes to a single stage fan with stator blades set at 64 degrees and rotor blades set at 30 degrees. 64-25-64-25 indicates two stage operation with identical stages; stator blades set at 64 degrees, rotor blades set at 25 degrees. X-30-64-30 referes to two stage operation

without [illegible] stage stator; second stage stator blades set at 64 degrees, rotor blades set at 30 degrees. Blade angles indicated are measured in the manner shown in Figure 8, page 19. All angles are measured at the midspan point of the blades.

Figure 9, page 20, illustrates the variation of static discharge pressure, static efficiency, and input horsepower with volume flow rate for single stage operation at constant speed with the rotor blades set at 20 degrees and stator blades at 54 degrees. This figure is an excellent example of the typical performance characteristics of vane-axial fans throughout the range from free delivery to shut-off. As the volume flow rate is reduced by the throttling device the discharge pressure increases rather rapidly to a peak value. Further reduction of the flow rate causes stalling, and instability of flow. This instability persists throughout the remainder of the low-capacity range, although the discharge pressure recovers after reaching some minimum value, and increases again right up to the shut off point.

After stalling occurs, the efficiency drops off rapidly. The input horsepower, which has decreased with the decrease in discharge pressure, realizes a slight increase in the unstable region and then assumes essentially the flat characteristic for which the axial fan is well known.

The stalling of the blades causes a more or less violent instability and oscillation of pressure and flow known as surging. This periodic flow and reversal of flow may take place gently, with instability of pressures as the only indication, or violently, with a series of loud

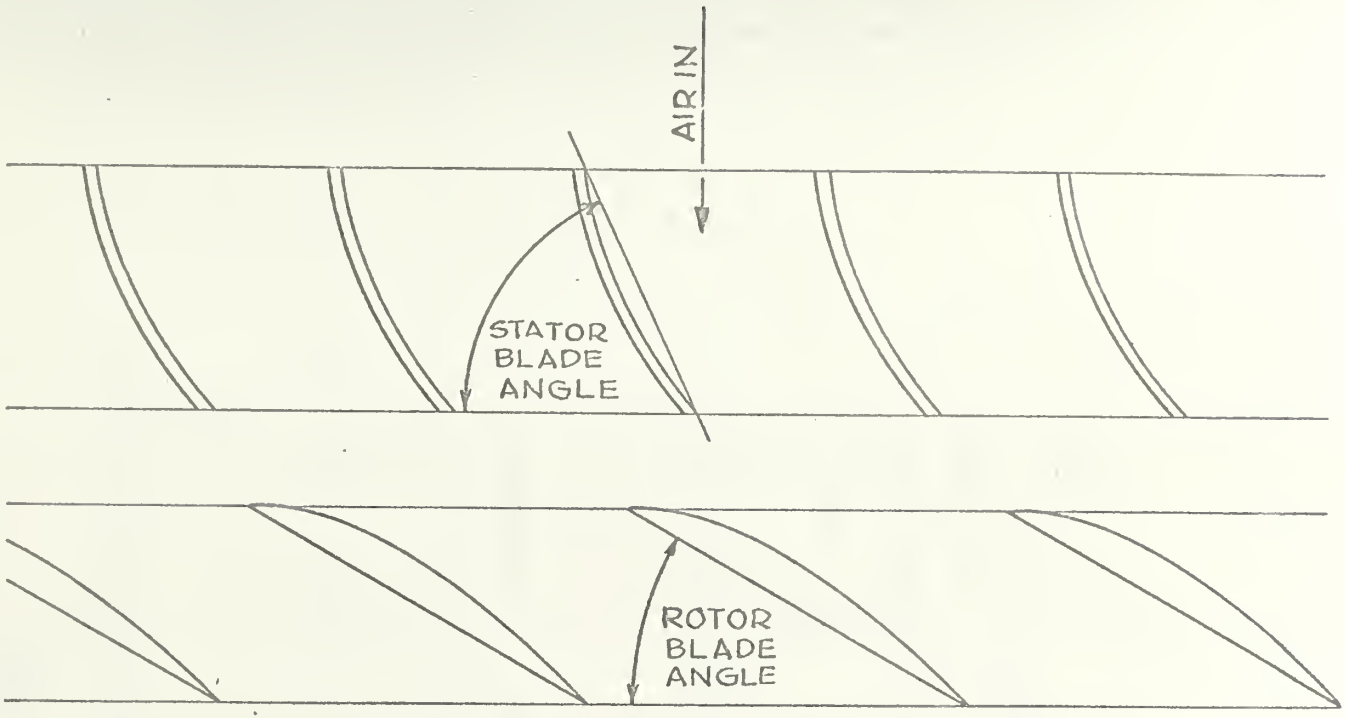

Figure 8. Method of measuring blade angles.

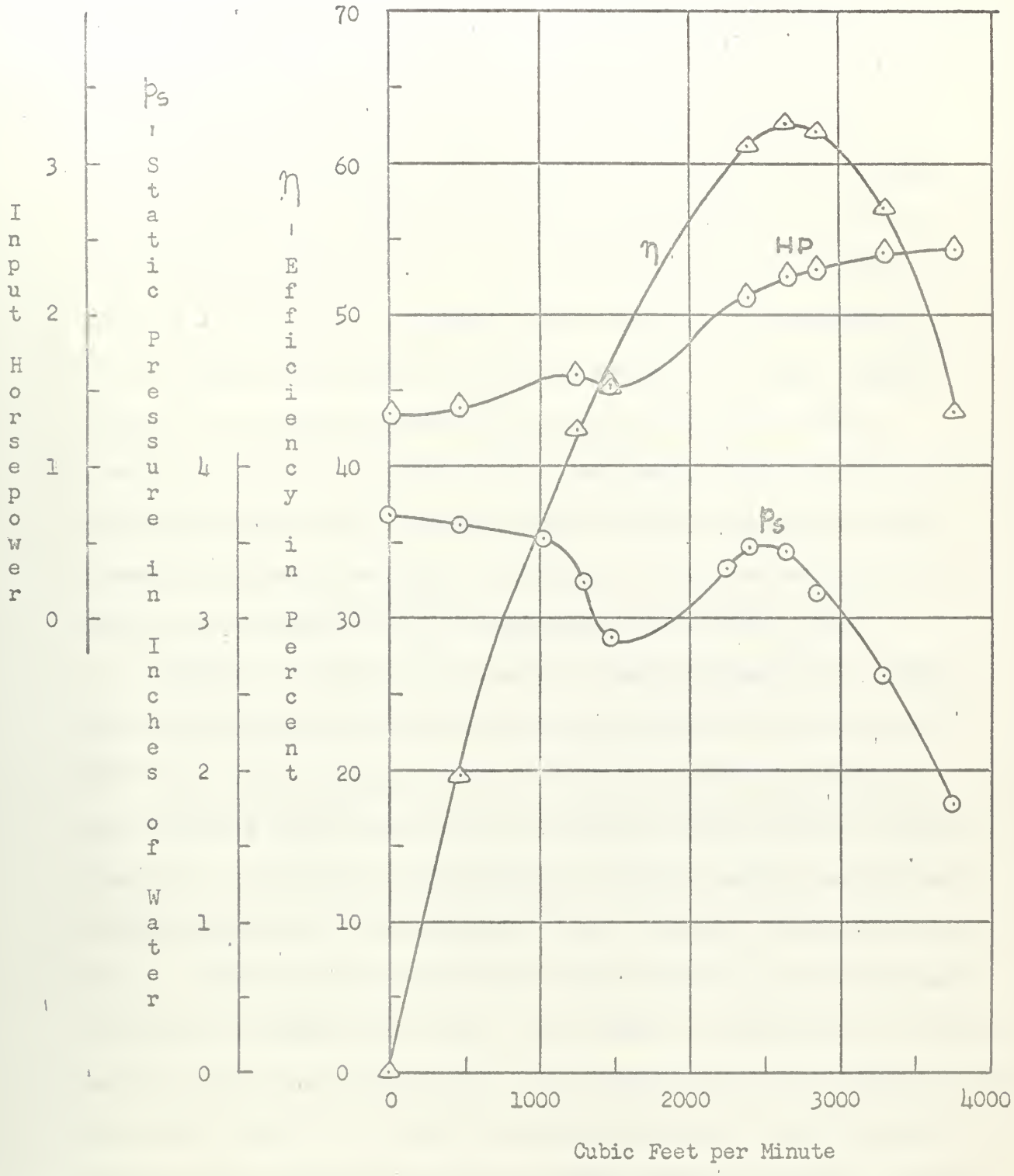

Figure 9. Performance characteristics of fan for single stage operation from free delivery to shut-off. Fan speed 2400 RPM. Blade angle settings 54-20.

bangs and fluctuations of pressure which can rapidly cause structural damage [5]. In addition, since operation of the fan in the surging condition results in low efficiency and high noise level, its operation should be limited to the range between peak pressure and free delivery to realize the efficient, quiet-operating characteristics of a well designed vane-axial fan [6]. On the basis of these remarks, the part of the characteristic to the left of the point of peak pressure is generally unusable, and in estimating characteristics, it is conservative to limit the usable part to that range between peak pressure and free delivery [5]. Because of this, the performance of the fan in this range only was investigated in all other tests.

Figures 11, 12 and 13 on pages 28, 29 and 30 respectively, illustrate the fan characteristics for two stage operation at a fan speed of 1800 RPM. Multi-staging of axial flow fans is generally employed to keep operating speeds and noise to a minimum for high pressure application [7]. In this fan, the available discharge pressure and the capacity increase as rotor blade angle. This, of course, is what one would expect. When both stator blades and rotor blades are in use, the degree of reaction is greater than unity. The degree of reaction may be defined as the ratio of the pressure rise in the rotor to the total pressure rise in a given stage [8]. When its value exceeds unity there is actually a slight loss in pressure in the stationary blades. Therefore, any rise in pressure must be explained by the conditions existing in the rotor. It can be shown that the pressure rise in a rotor is proportional to both the axial velocity through the rotor and the change of the whirl components

of the relative velocities into and out of the rotor. With constant stator blade angle the inlet whirl component remains fixed. However, as the rotor blade angle increases from 20 degrees to 40 degrees, the whirl component leaving the rotor decreases. This may be readily seen in the velocity triangles shown in Figure 10a on page 23. These velocity triangles, comparing conditions for rotor blade angles of 20 degrees and 40 degrees, were constructed using the known values of the angle of the relative velocity vector, W leaving the rotor blade, the peripheral speed, U and the axial velocity component, V_a . This latter quantity was determined by a measure of the velocity pressure by the total pressure probe in the discharge duct while the fan was operating in the free delivery condition. Naturally, the value determined in this manner is not exactly equal to the velocity at the rotor, because of losses, but it is close enough to demonstrate the action.

For a constant value of the whirl velocity going into the rotor then, the pressure rise increases with decreasing value of the whirl component out and with increasing axial velocity. Actually, this is only a qualitative analysis of the phenomenon, but it is sufficient for the scope of this work.

In a like manner, the volume flow rate varies as the axial component of the velocity out of the fan since $Q = AV_a$. Therefore, with greater rotor blade angles and subsequent higher densities and larger values of the axial velocity, greater capacities are realized.

The power delivered to the fan is likewise dependent on the change of whirl components across the rotor. Therefore, by a similar analysis as that used to explain the higher pressures, we can also explain

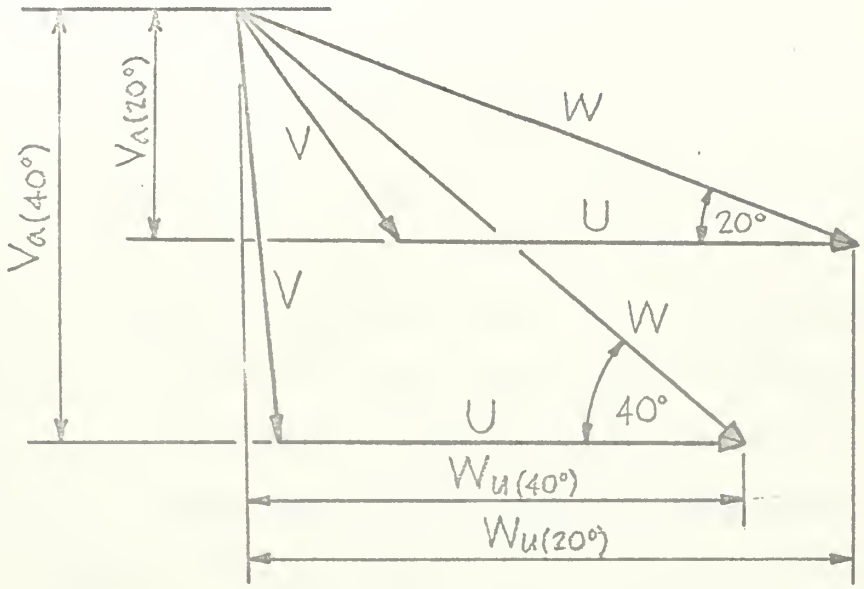

Figure 10a. Comparison of whirl components W_u of relative velocity vectors W leaving rotor blades while fan in free delivery condition for two different rotor blade angles.

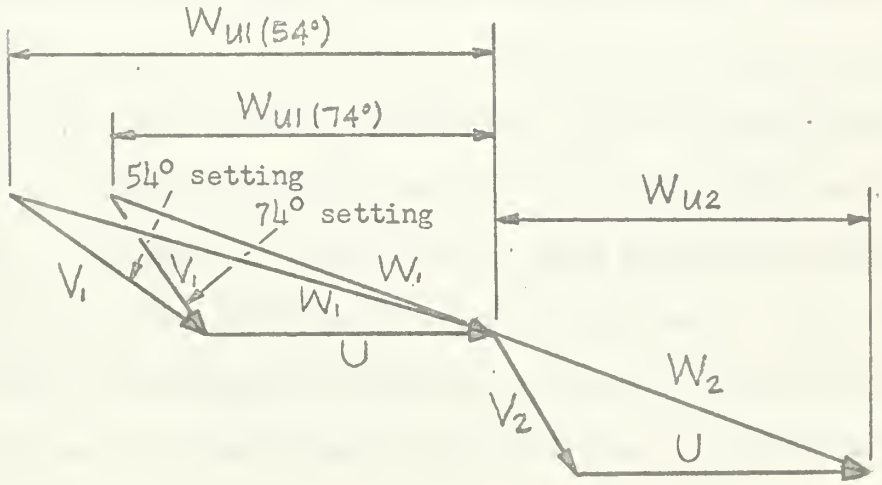

Figure 10b. Comparison of whirl components W_{u1} of relative velocity vectors W_1 entering rotor blades while fan delivering equal flow rates for two different stator blade angles.

the higher values of input horsepower required for the larger rotor blade angles.

In Figures 14, 15 and 16 on pages 31 , 32 and 33 respectively, are shown the effects of increasing the number of stages in the fan while maintaining its speed at a constant value. We see that for stator blade angles of 64 degrees and rotor blade angles of 30 degrees, the discharge pressure is doubled by adding an additional stage to the single stage fan. Again, the axial component of the velocity out of the fan is greater in the two stage operation than with the single stage, yielding greater capacity for volume flow rate. As is to be expected, the ratio of the flow rates for the two conditions at free delivery is almost exactly equal to the ratio of the axial velocities.

Not only is the peak pressure doubled when adding a second stage, but so is also the required input horsepower. The work added in each stage should be approximately equal, so this would, therefore, be a logical result. It should be noted that for equal volume flow rates, the two stage fan is more efficient than the single stage. This is due to the fact that the percentage increase in pressure realized with the addition of the second stage slightly outweighed the percentage increase in power required.

Turning to the comparison of the two stage fan without inlet guide vanes, with the single stage operation with rotor only, we see that the addition of another rotor with guide vanes between the two stages, again doubles the pressure available at any flow rate. Also, for a given system resistance, it makes possible higher flow rates because of this

fact. This, of course, is true of the previous comparison made, also.

It developes that the additional power required for the added stage is great enough to lower the efficiency of the two stage fan without inlet guide vanes below that of the single stage for a considerable portion of its useful range.

Using the results shown in Figures 14, 15 and 16, pages 31, 32 and 33, we can also draw some conclusions about the operation of fans, single and two stage, with and without inlet guide vanes. For instance, for two stage operation we find that the addition of inlet guide vanes to a fan without them will raise the available pressure and increase the capacity under free delivery by about 19 per cent from 3700 CFM to 4400 CFM. This calls for an increase of power input, but results in overall operation considerably more efficient (about 14 per cent) than that without the first stage stator vanes. The increased efficiency may be attributed to the air being directed against the rotor blades in the first stage at a much more favorable incidence due to the guide vanes.

In like manner, the presence of inlet guide vanes in the single stage fan raises the available pressure over that obtainable without the stator blades, and increased capacity is realized. The incidence of the incoming air upon the moving blades when guide vanes are absent is such to probably cause separation at the higher flow rates with resulting loss of pressure and efficiency even though the efficiencies for both types of operation appear to peak at the same value (but different flow rates). The results of these two methods of operation serve to illustrate the difference between the characteristics of tube-axial and vane-axial fans. Tube-axial fans are those axial flow fans provided with

a casing of some type in which the rotor turns but in which there are no stationary blades. Vane-axial fans are similar to tube-axial fans except that they are provided with stationary blades or vanes either before or after the rotor.

The comparison of the basic quantities for single stage operation with various rotor and stator blade angles is shown in Figures 17, 18 and 19 on pages 34, 35 and 36 . First, the effect of varying the stator blade angle with constant rotor blade angle will be discussed. It is apparent for both rotor blade angles shown, that as the stator blade angle is decreased the capacity increases, as does the pressure available at any given flow rate. The reasons for this can be clearly seen by studying the velocity triangles shown in Figure 10b, page 23. These triangles indicate the nature of the flow for rotor blade angle settings of 20 degrees and stator blade angle settings of 54 and 74 degrees. For equal flow rates, or in other words equal axial velocities, it is obvious that the change in whirl components for the 54 degree setting is considerably greater than that for the 74 degree setting. Of course, the 64 degree setting would fall between the two. Thus, for equal flow rates, the 54 degree setting produces the highest pressure of the three settings.

For equal pressures, we see that the 54 degree setting produces the highest flow rate. This is due to the fact that since this blade setting is capable of producing higher pressures it can push more flow through the system, the resistance of which increases with volume flow. Expressed another way, since higher pressures are available, the system resistance limits the flow at a higher flow rate.

For a given setting of the stator blades, the variation of the characteristics for increasing rotor blade angle is easily explained with the same arguments as used in the case of two stage operation earlier, since we see that, in like manner, the pressure available and the capacity increase with increasing rotor blade angle.

The explanations for the performance characteristics presented thus far apply only to the range of blade angles and stage combinations tested, naturally. One could not expect to obtain higher pressures and capacities indefinitely merely by increasing rotor blade angle, for instance. At some point this trend would, of course, reverse itself when the flow conditions in the fan ceased to improve and again worsened.

Typical performance characteristics similar to those shown in Figures 11 through 19, pages 28 through 36 , are provided by the manufacturer in the instruction book. The curves provided, however, are not guaranteed, and except to mention a similarity, there is no point in making a comparison of the characteristics determined here with those provided.

In Figures 20 and 21, pages 37 and 38, the performance of the fan both as a single stage and a two stage unit at various fan speeds is shown. These figures are good examples of typical axial flow compressor "maps". The lines connecting the stall points represent the "surge lines" or the limiting boundaries to the usable ranges of the fans. The points at the other ends of the constant speed lines represent the limits of flow obtainable. That is, for the speed concerned, no higher flow rate can be produced through the system.

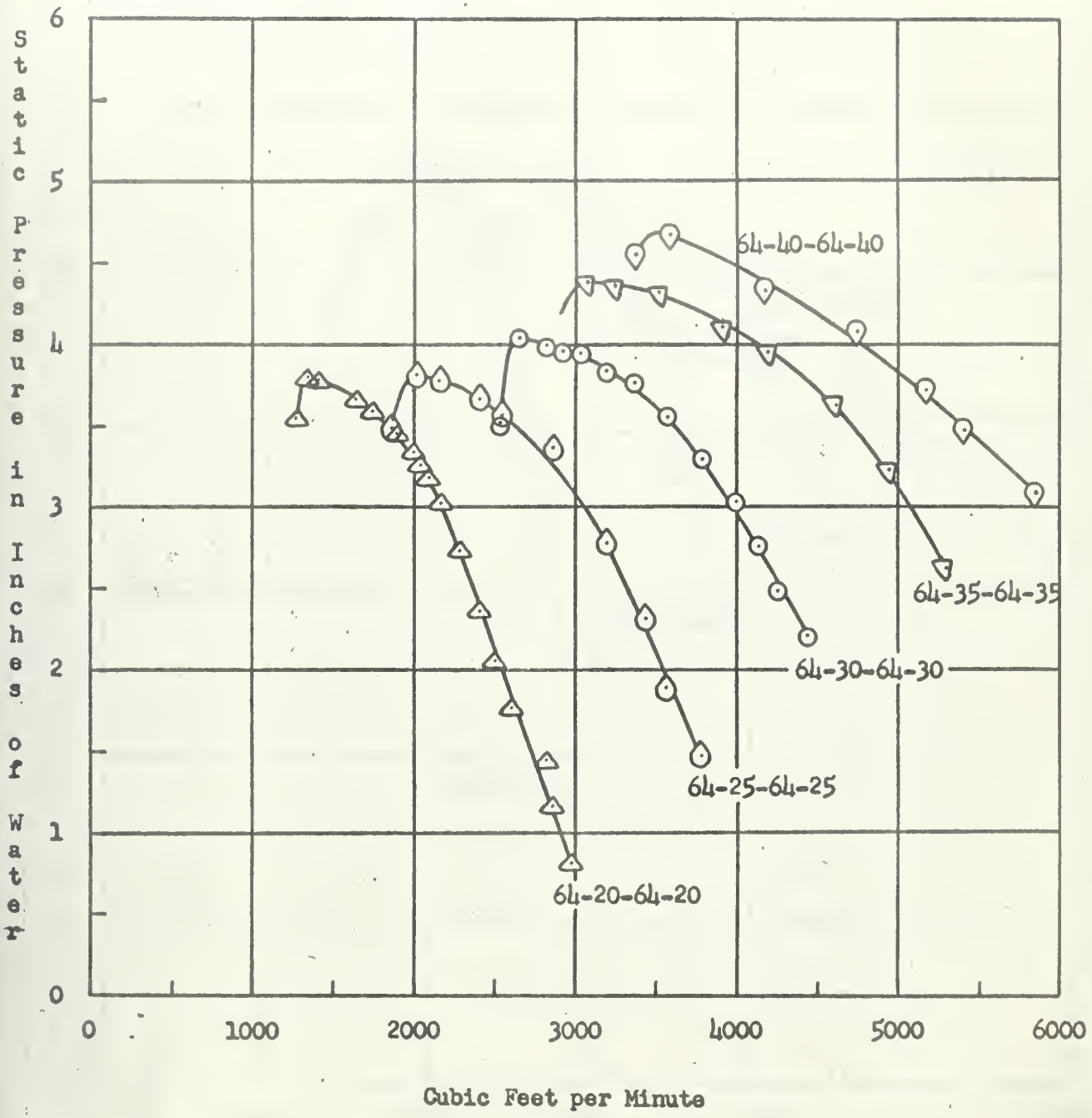

Figure 11. Variation of static discharge pressure with volume flow rate for various rotor blade angles. Fan speed 1800 RPM. Two stage operation.

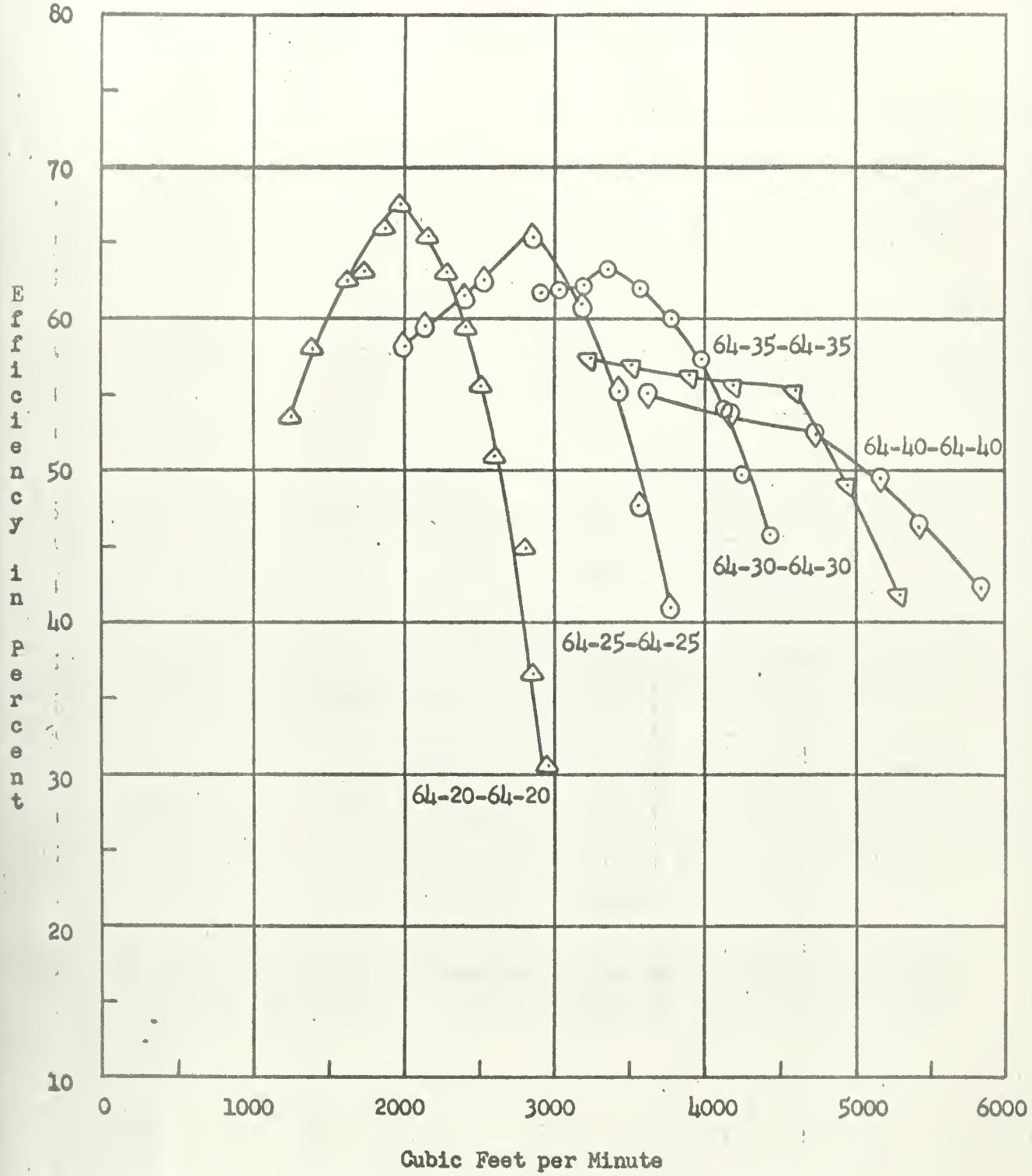

Figure 12. Variation of static efficiency with volume flow rate for various rotor blade angles. Fan speed 1800 RPM. Two stage operation.

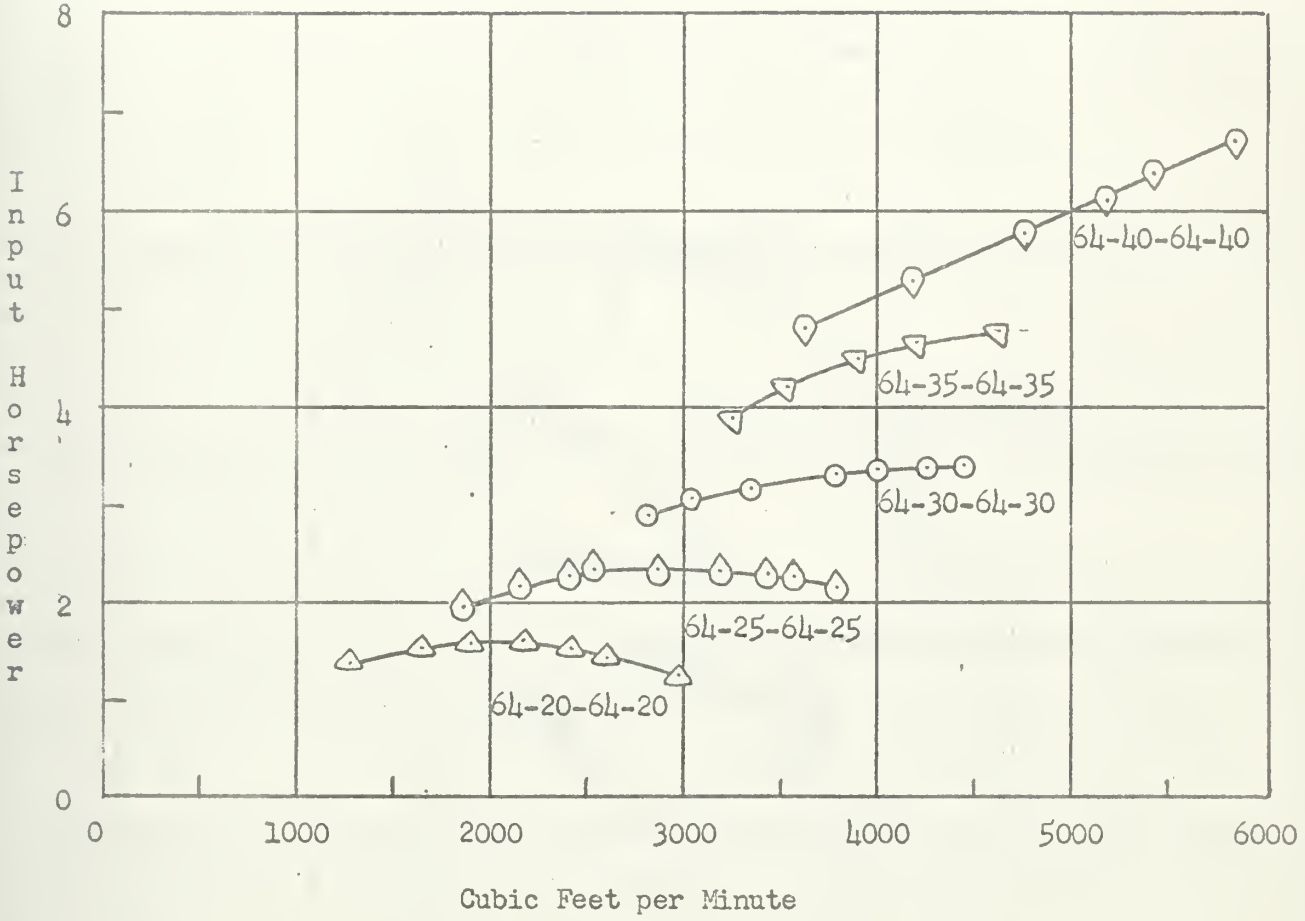

Figure 13. Variation of input horsepower and volume flow rate for various rotor blade angles. Fan speed 1800 RPM. Two stage operation.

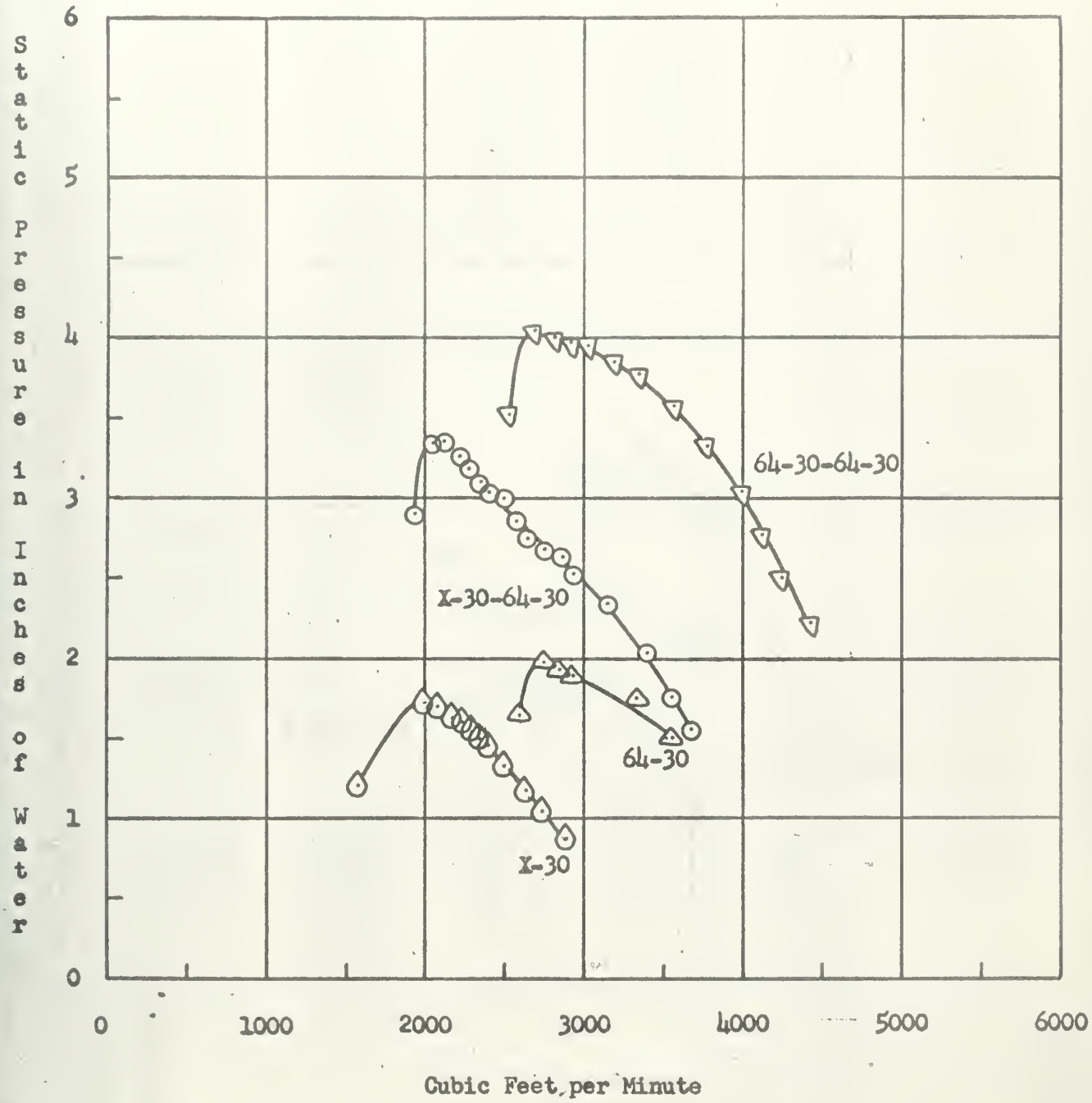

Figure 14. Variation of static discharge pressure with volume flow rate for various stage combinations. Fan speed 1800 RPM.

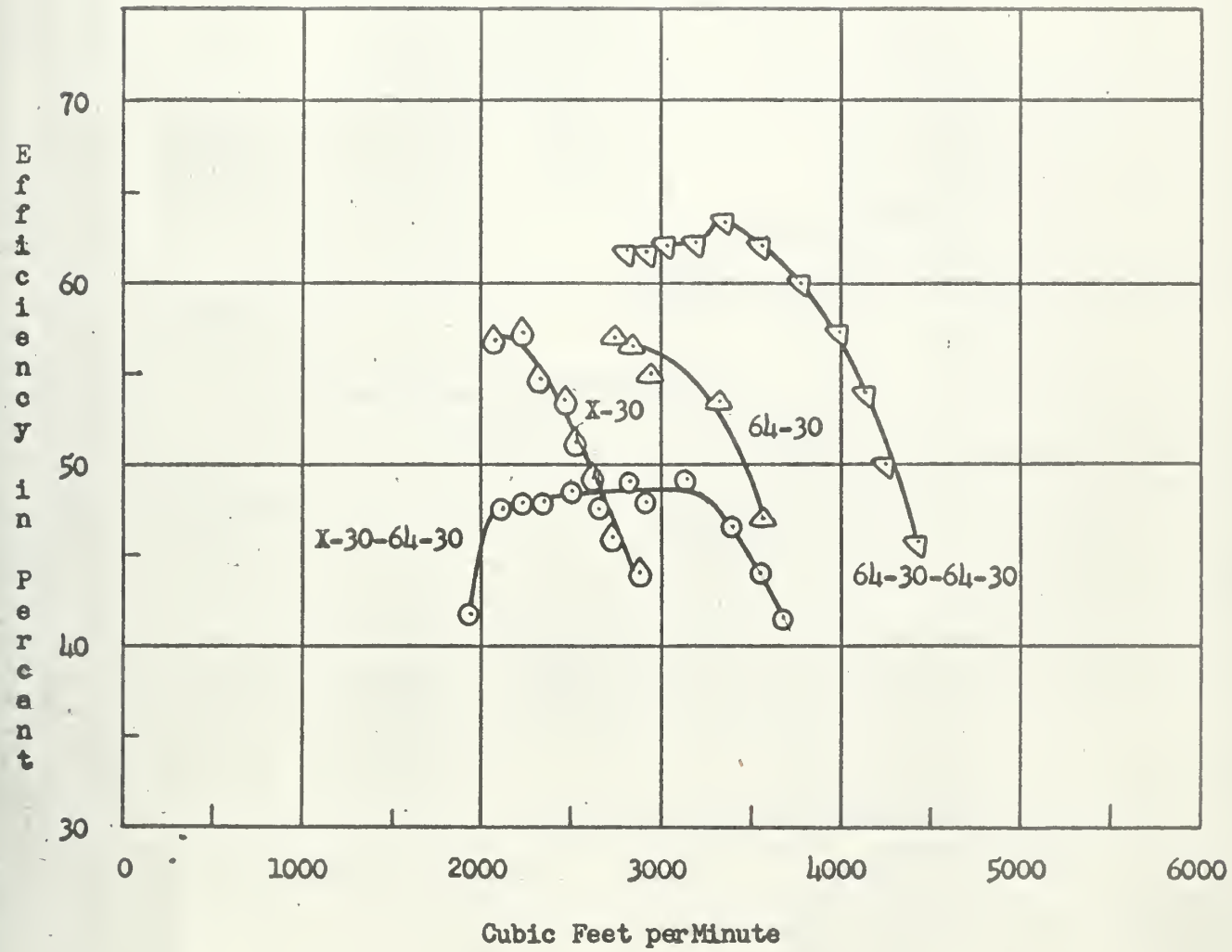

Figure 15. Variation of static efficiency with volume flow rate for various stage combinations. Fan speed 1800 RPM.

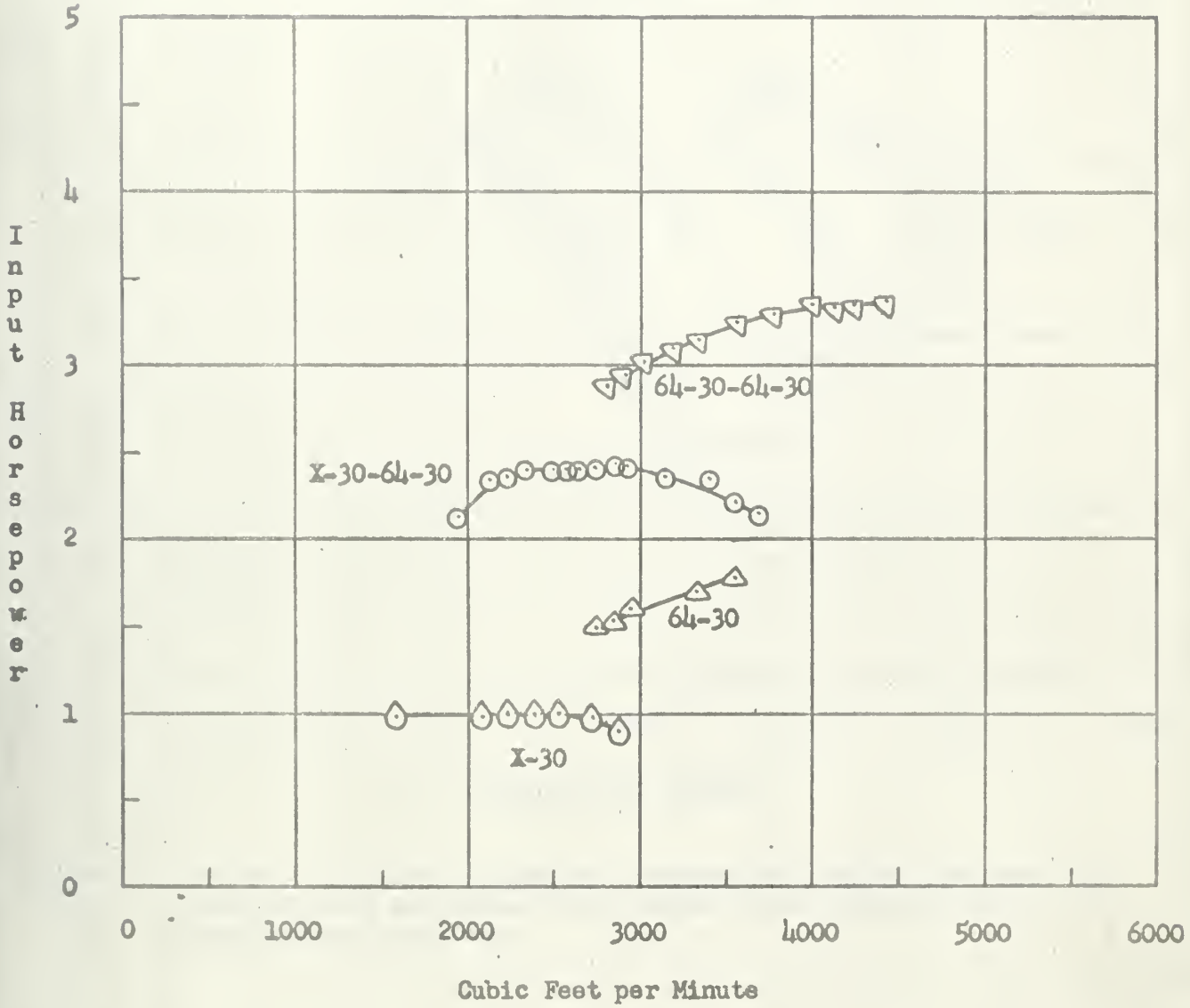

Figure 16. Variation of input horsepower with volume flow rate for various stage combinations. Fan speed 1800 RPM.

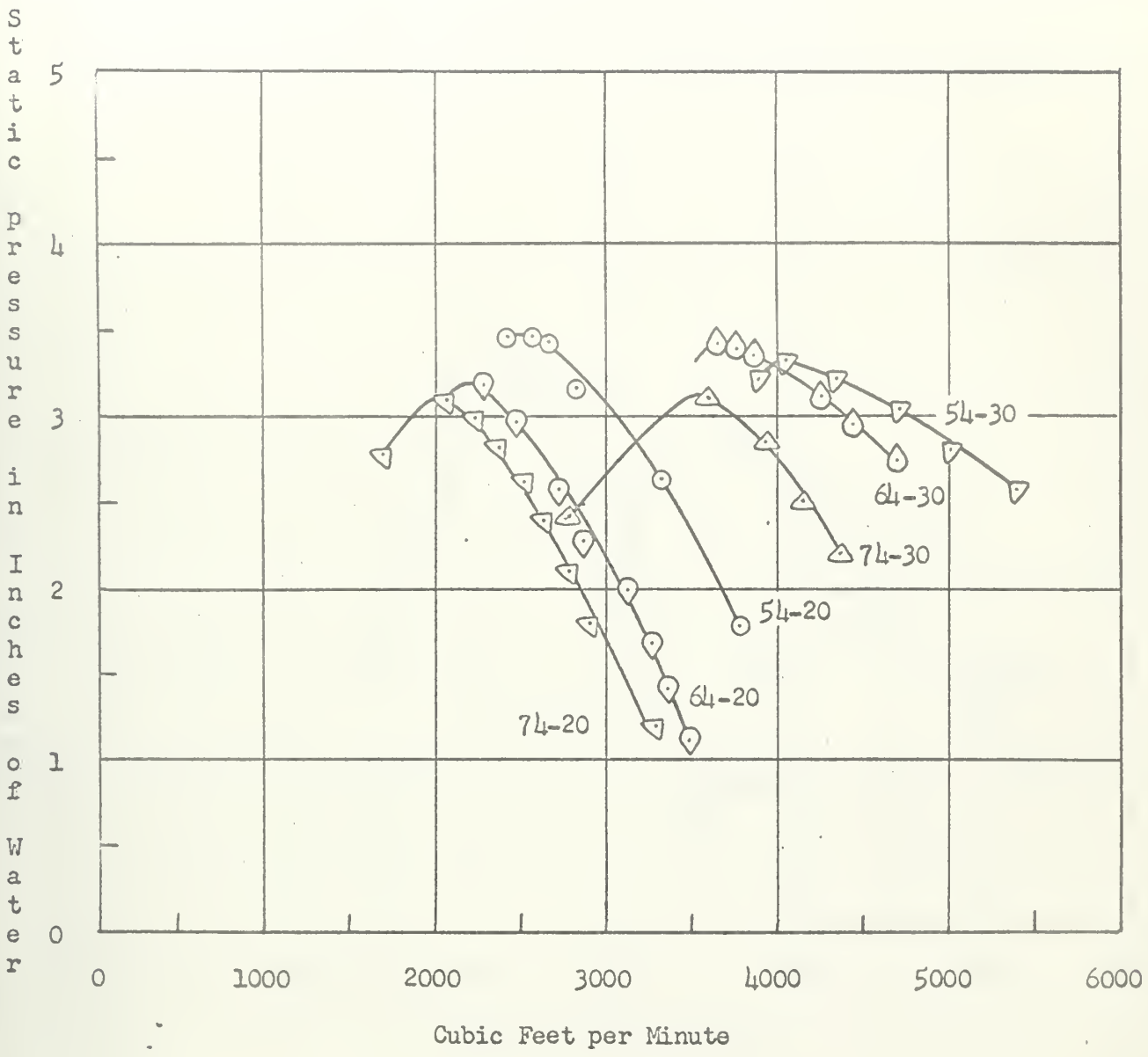

Figure 17. Variation of static discharge pressure with volume flow rate for various rotor and stator blade angles. Fan speed 2400 RPM. Single stage operation.

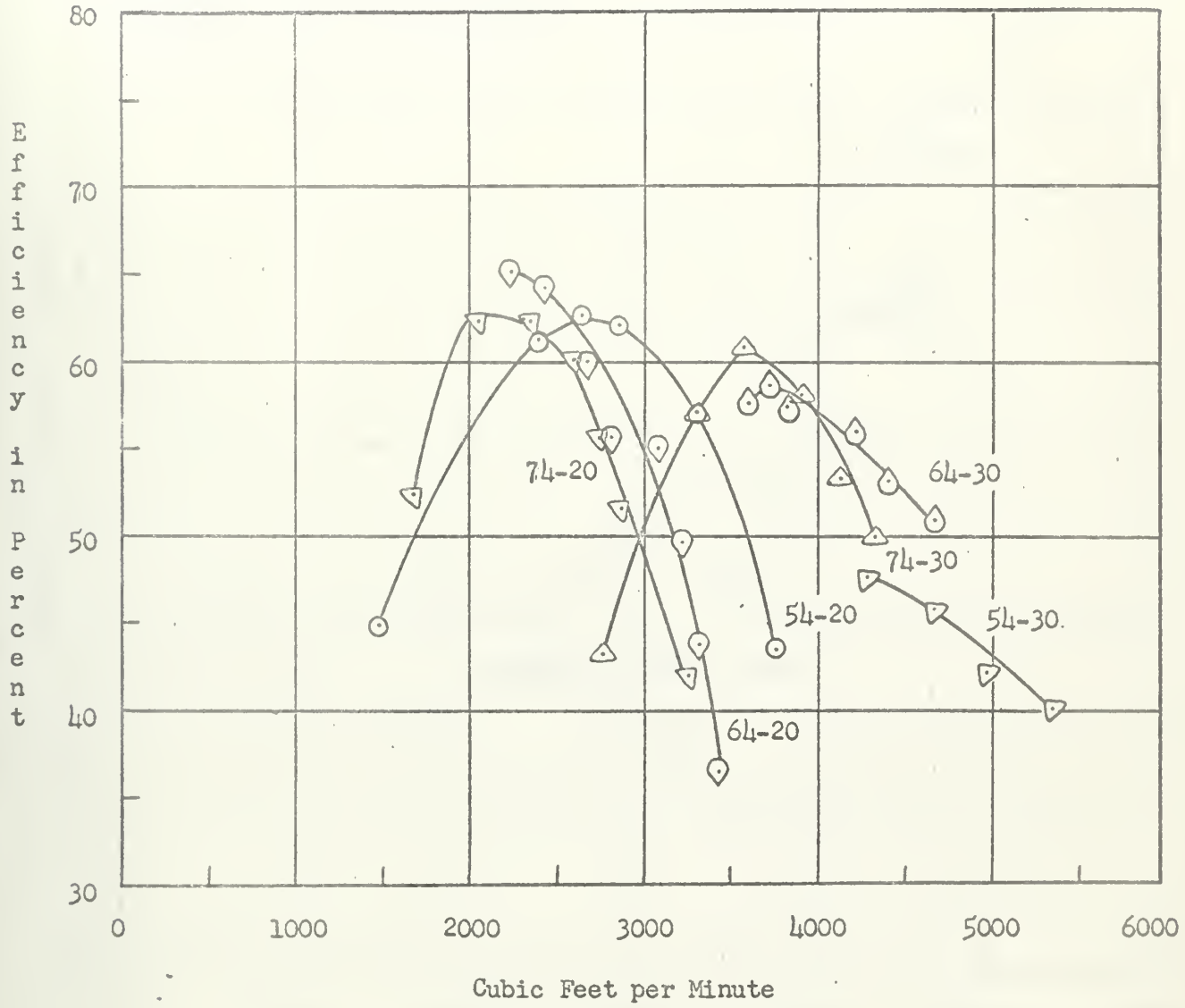

Figure 18. Variation of static efficiency with volume flow rate for various rotor and stator blade angles. Fan speed 2400 RPM. Single stage operation.

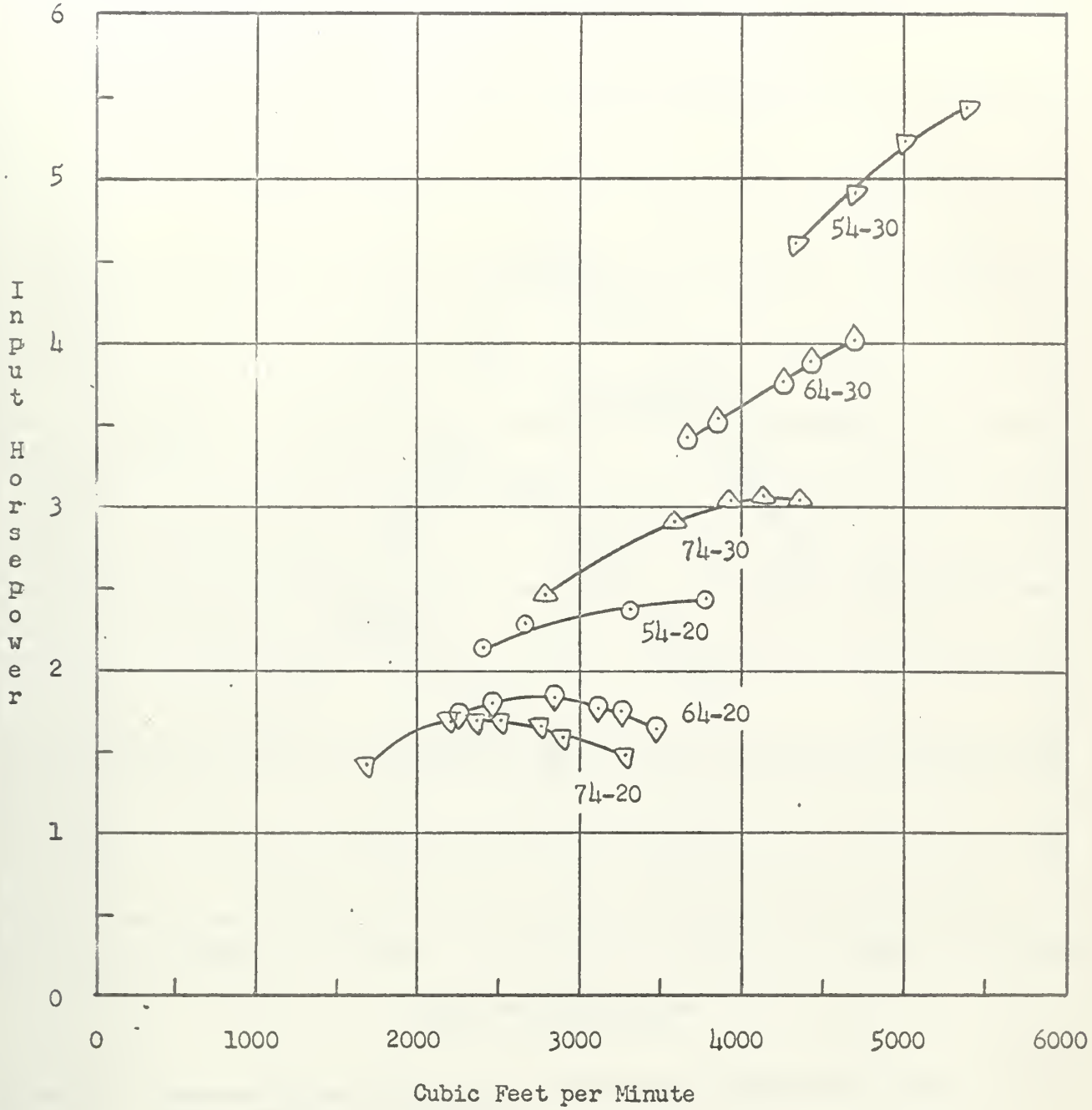

Figure 19. Variation of input horsepower with volume flow rate for various rotor and stator blade angles. Fan speed 2400 RPM. Single stage operation.

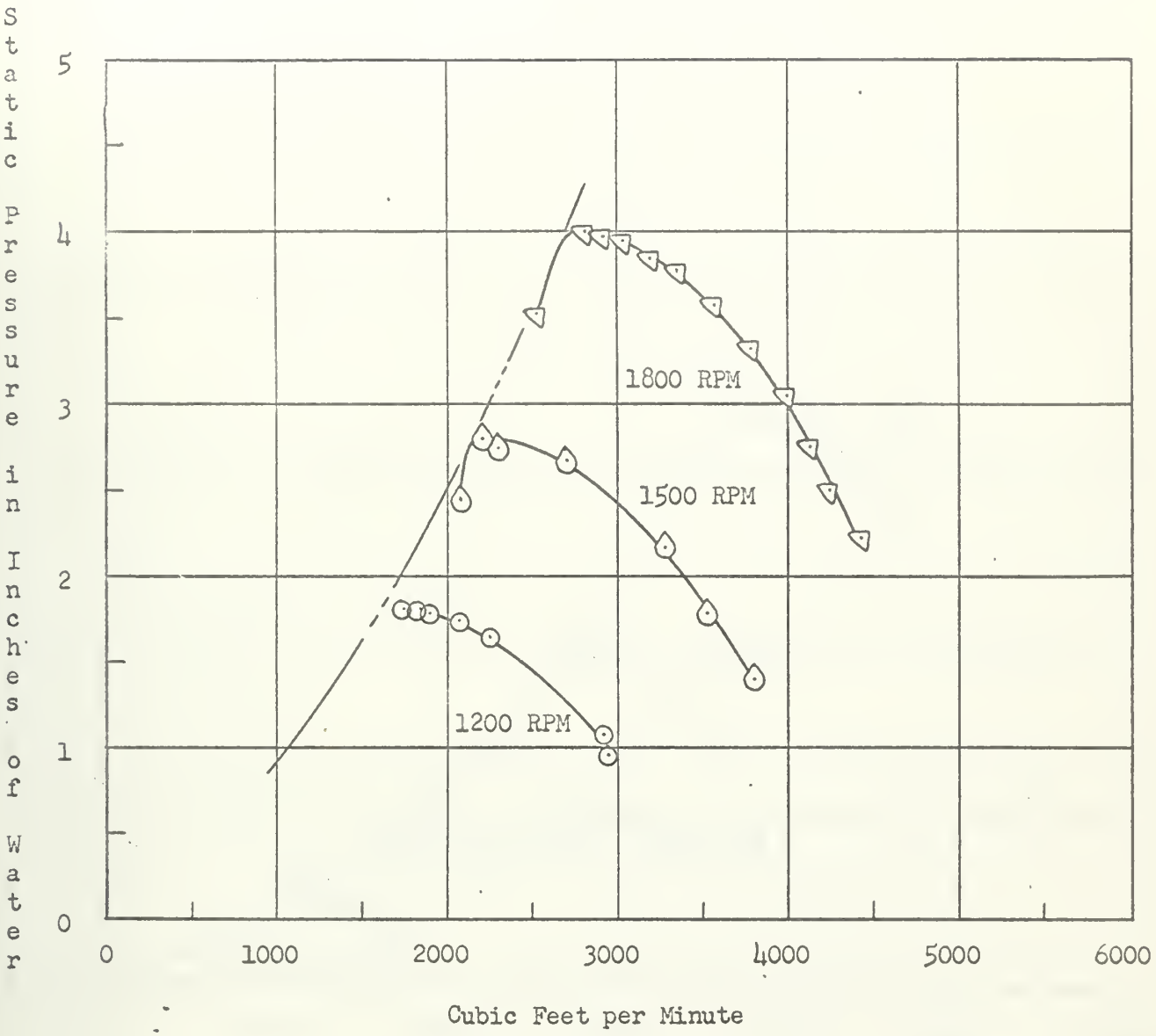

Figure 20. Characteristics of two stage operation at various fan speeds. Blade settings 64-30-64-30.

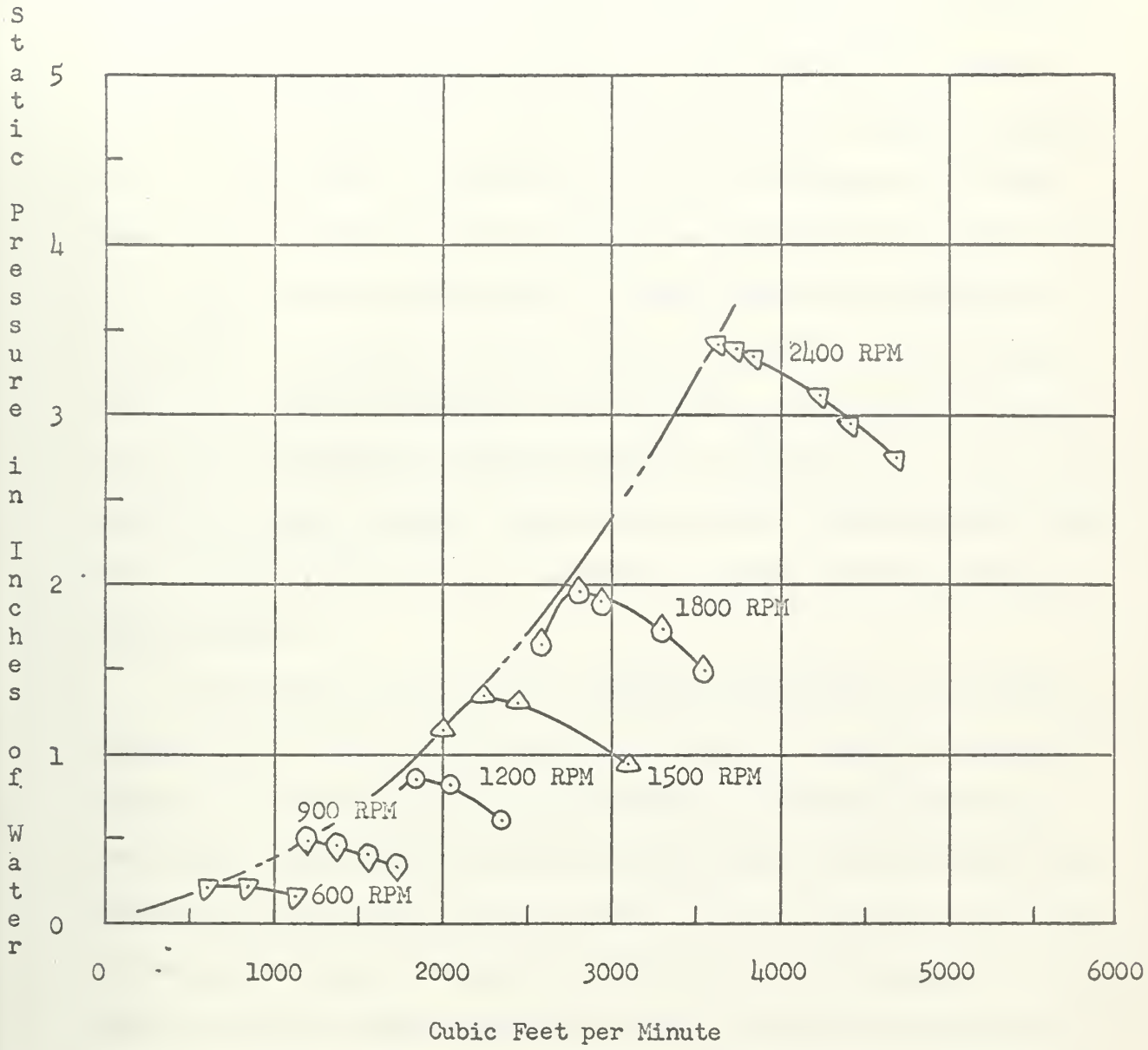

Figure 21. Characteristics of single stage operation at various fan speeds. Blade settings 64-30.

7. Conclusions and Recommendations.

The installation of the equipment has been completed. Sufficient testing has been performed to be able to conclude that the existing facilities are adequate for use of the fan set-up for laboratory instruction. A wide range of characteristics of the performance of the fan under varying operating conditions have been obtained and recorded.

In the opinion of the writer, it would seem to be of interest in the future to fabricate different types of blades for use in the fan. This would offer the advantage of being able to demonstrate the performance of fan stages with different degrees of reaction, i.e., 50 per cent reaction and zero reaction. Naturally, this would call for careful attention to the operation of the machinery to ensure that the equipment is not overloaded.

In the use of the set-up for laboratory instruction, it is recommended that a minimum of four hours be allotted for any given group of students. At least two hours would probably be needed to allow for preliminary instructions and the recording of data for a particular fan set-up at perhaps three different speeds. If it is desired to run tests for varying set-ups, a minimum of 1-1/2 hours should be planned for change-over of the fan. These considerations will, of course, be dependent on the type of instruction planned.

8. Bibliography

1. General Electric publication No. GEI-48919E. Instruction Book for Model 5GDY34C1 Axial Flow Fan-Dynamometer Set.

2. PTC 11-1946. A.S.M.E. Power Test Code for Fans.

3. PTC 19.5; 4-1959. A.S.M.E. Supplement to Power Test Codes on Flow Measurement, Chapter 4, Part 5.

4. Theodore Baumeister, Jr., "Fans", McGraw-Hill Book Co., Inc., 1935.

5. D. G. Shepherd, "Principles of Turbomachinery", The MacMillan Co., 1956.

6. Kent's Mechanical Engineer's Handbook, Power Volume, 12th Edition.

7. A. N. Rogers, "Features of Axial Flow Fans", Air Conditioning, Heating and Ventilating magazine, Jan. 1958.

8. M. H. Vavra, "Aero-Thermodynamics and Flow in Turbomachines", John Wiley and Sons, Inc., 1960.

APPENDIX A

1. Air Flow Calculations.

The flow metering nozzles in the plenum chamber were used to determine the volume flow rate from the fan. Before this could be done, however, it had to be established that the nozzles would indicate the flow rate accurately. This was done by obtaining the flow rate from velocity surveys at the throat of the nozzles as mentioned in Section 6, and comparing these results with the flow rates indicated by the pressure differential across the nozzles.

Reference [3] describes the method of determining volume flow rate for A.S.M.E. long radius nozzles. The mass rate of flow, w_H in pounds per hour is determined by

$$w_H = 359 C F d^2 F_a Y_a \sqrt{h_w \rho} \qquad (1)$$

where C is the nozzle discharge coefficient, F is the velocity of approach factor (equal to unity in this case), d is the diameter of the nozzle, F_a is the nozzle thermal expansion factor (also equal to unity), Y_a is the adiabatic expansion factor, which may be considered to have a constant value of 0.999 with negligible error, h_w is the differential head across the nozzle in inches of water at 68F, and ρ is the air density in pounds per cubic foot. The volume flow rate, Q in cubic feet per minute can now be determined by

$$Q = \frac{w_H}{60\rho} \qquad (2)$$

Reference [3] points out that if the throat Reynolds number exceeds 200,000 the discharge coefficient may be considered equal to 0.99. This means then, that

$$Q = \frac{359 \times .99 \times 1.0 \times d^2 \times 1.0 \times .999 \sqrt{h_w \rho}}{60 \rho} = \frac{5.92 d^2 \sqrt{h_w}}{\sqrt{\rho}} \quad (3)$$

If the density ρ is taken to be the standard density of .075 pounds per cubic foot,

$$Q = 21.6 d^2 \sqrt{h_w} \quad (4)$$

or for a given nozzle diameter it is equal to the product of a constant and the square root of the differential head.

$$Q = K \sqrt{h_w} \quad (5)$$

Taking logarithms of both sides of equation (5), we have

$$\ln Q = \ln K + \tfrac{1}{2} \ln h_w \quad (6)$$

If this relationship is plotted on a logarithmic graph a straight line with a slope of 1/2 is obtained. If the value of the constant is determined for each nozzle and each combination of nozzles used, a family of straight lines representing these combinations may be plotted.

This type of presentation is shown in Figure 22, page 44. The experimental points indicated represent the actual values of flow rate as determined by the velocity traverses at the nozzle throats. It was found that the curves would accurately predict the flow rate for all cases except for the combination of the two large nozzles in use at once. In this case, the slope of the line on the logarithmic plot apparently is not equal to 1/2. Therefore, the three experimental points obtained for this combination were used to establish a calibrated curve which can now be used to determine the flow rate for a given differential head.

For the two small nozzles, the range in which the throat Reynolds number exceeds 200,000 is quite limited, as indicated. However, the experimental data for these nozzles appears to indicate that their usable

range extends to include Reynolds numbers less than 200,000.

The numbered designations of the nozzles are indicated in Figure 23 on page 45.

The volume flow rate from the fan at a given plane varies directly as the speed. When the test speed is not exactly constant throughout a run, or when it differs slightly from the value desired, the volume flow rate must be corrected by the factor n_s/n_x where n_s is the specified speed, and n_x is the test speed.

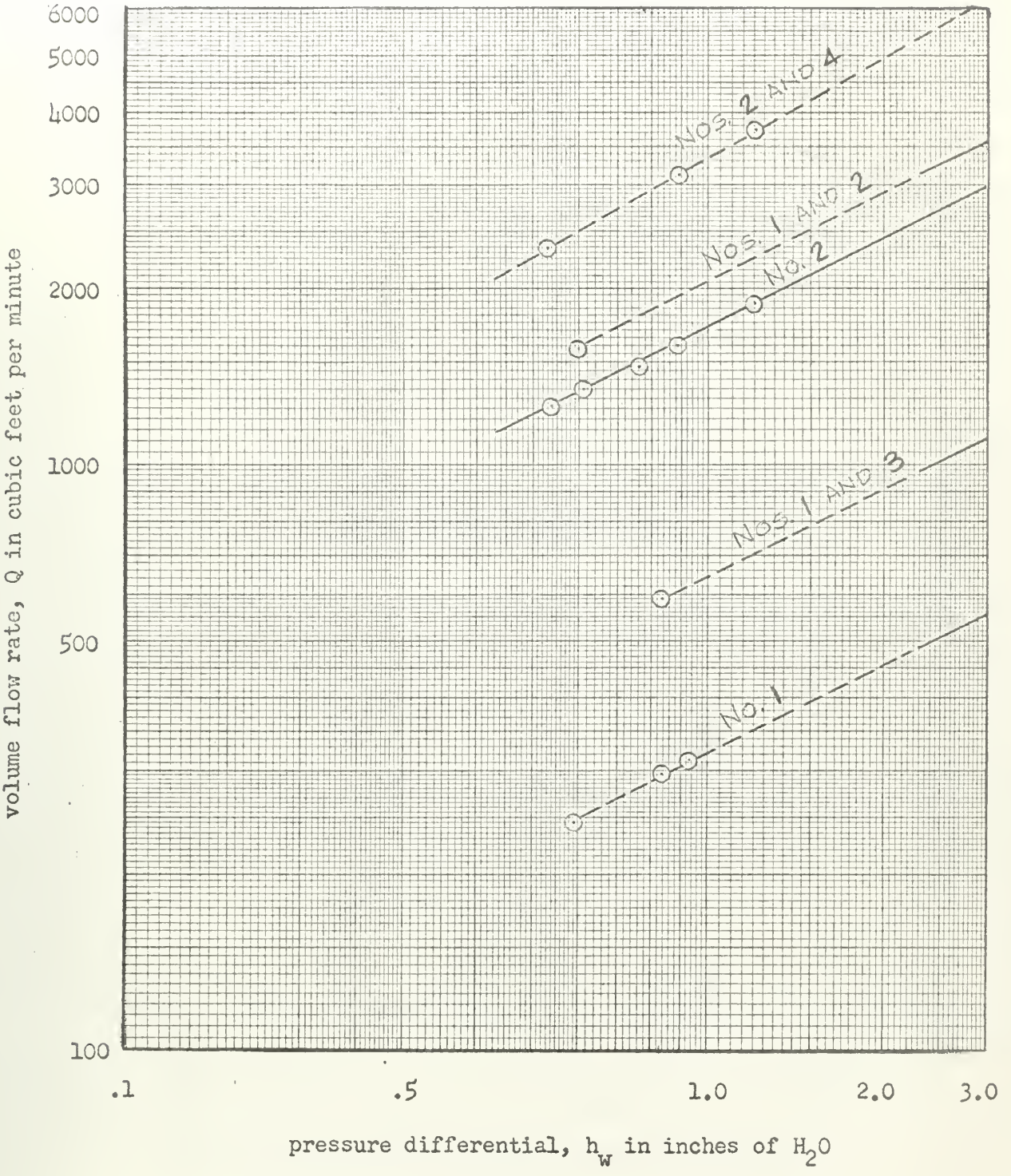

Figure 22. Variation of volume flow rate with pressure differential across flow metering nozzles. Solid lines indicate variation predicted theoretically, dashed lines indicate variation established experimentally.

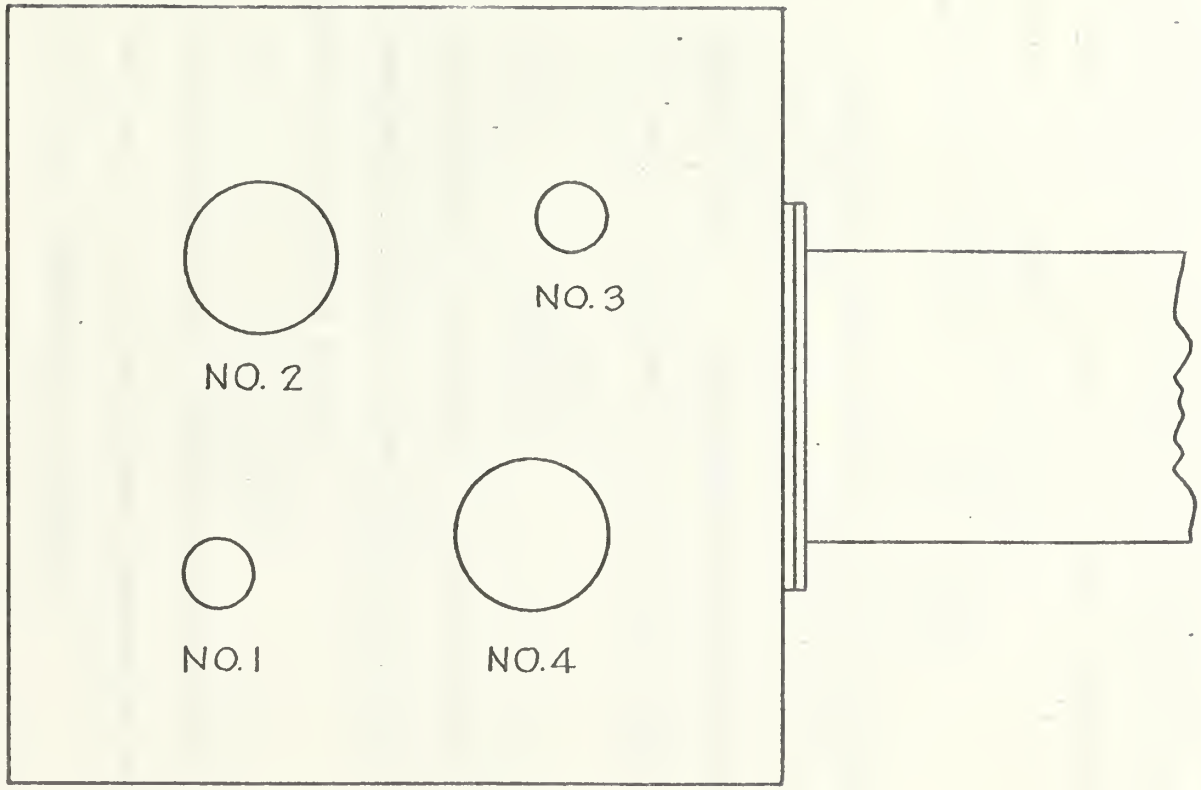

Figure 23. Designations of flow metering nozzles.

2. Discharge Pressure Correction.

For a given position of the throttling device, the pressure at any point in the duct varies as the square of the speed and directly as the density at that point. The fan static discharge pressure must therefore be corrected for varying speed and density.

$$\text{Pressure correction factor} = \left[\frac{n_s}{n_x}\right]^2 \times \left[\frac{\rho_s}{\rho_x}\right]$$

where ρ_s is taken as the density of dry air at 70F and 29.92 inches (equal to 0.07494 pounds per cubic foot), ρ_x is the air density at the fan inlet during the test, n_s is the specified speed, and n_x is the test speed. ρ_x may be determined in the following manner.

$$\rho_x = \frac{p_a - (.38)p_p}{.754\ T_a}$$

where p_a is the barometric pressure in inches of mercury at 32F, T_a is the air temperature in degrees F abs, p_p is the partial vapor pressure in the atmosphere in inches of mercury.

$$p_p = p_g - \frac{p_a(t_a - t_w)}{2700}$$

where p_g is the saturated vapor pressure at the wet-bulb temperature in inches of mercury, t_a is the dry-bulb temperature in degrees F and t_w is the wet-bulb temperature in degrees F.

APPENDIX A

3. Power Input Calculations.

The power input delivered to the fan coupling may be calculated by the following equation.

$$HP_{in} = \frac{T\omega}{33{,}000} = \frac{2\pi nWL}{33{,}000} \qquad (8)$$

where L is the length in feet of the dynamometer torque arm from shaft center to knife edge, W is the force in pounds measured at distance L, and n is the speed in revolutions per minute. Since the dynamometer torque arm is equal to 1.31 feet, equation (8) simplifies to

$$HP_{in} = \frac{Wn}{4000} \qquad (9)$$

Power input varies as the cube of the speed and directly as the density. Therefore, the calculated horsepower must be corrected for varying speed and air density.

$$\text{Power correction factor} = \left[\frac{n_s}{n_x}\right]^3 \times \left[\frac{\rho_s}{\rho_x}\right]$$

where the symbols have the same meanings as in the previous sections.

APPENDIX A

4. Static Efficiency Calculations.

The static efficiency of the fan compares the output power to the input power. The product of volume flow rate and pressure yields the output power. Input power is as determined by the dynamometer.

$$HP_{out} = Q \times p_s \left[\frac{14.69 \times 144}{13.6 \times 29.92 \times 33{,}000}\right] = \frac{Q \times p_s}{6356} \qquad (10)$$

$$\eta_s = \frac{HP_{out}}{HP_{in}} = \frac{Q \times p_s}{6356\, HP_{in}} \qquad (11)$$

where η_s is the static efficiency, Q is the volume flow rate in cubic feet per minute, and p_s is the fan static discharge pressure in inches of water. The quantities Q, p_s, and HP_{in} are all as corrected to specified speed and density as described in the previous sections.

APPENDIX B

Sample calculations.

The calculations shown in this appendix constitute a sample of those required in the determination of the characteristics described in earlier sections. The input data for these calculations were obtained from operation of the fan with a single stage at 2400 RPM. Stator blades were set at 54 degrees, and rotor blades were at 20 degrees. Results of the calculations are tabulated here and shown in graphical form in Figure 24 page 52.

Recorded data.

Run	n	W	p_s	h_w	NOZ
1	2400	4.05	1.76	1.19	2,4
2	2410	4.05	2.63	0.92	2,4
3	2410	3.85	3.16	0.69	2,4
4	2410	3.80	3.42	0.58	2,4
5	2410	3.55	3.45	0.48	2,4

n is fan speed, RPM

W is force on dynamometer torque arm, pounds

p_s is static discharge pressure, inches of water

h_w is differential head across flow nozzles, inches of water

NOZ is the nozzle combination in use

t_1 = air dry-bulb temperature = 71F

t_w = air wet-bulb temperature = 61F

barometric pressure = 30.30" Hg

air temperature at barometer = 71 F

APPENDIX B

Sample calculations are for run No. 1.

(1) Determine Q from Figure 22, page 44.

$$Q = 3710 \text{ CFM}$$

(2) Correct Q for specified speed.

$$Q = 3710 \times \frac{n_s}{n_x} = 3710 \times \frac{2400}{2400} = 3710 \text{ CFM}$$

(3) Determine ρ_x.

$$P_j = .5407 \text{ "Hg}$$

correct P_A to 32F using barometer correction tables.

$$P_A = 30.30 - .135 = 30.165 \text{ "Hg at 32F}$$

$$P_p = .5407 - \frac{30.165(71-61)}{2700} = .4287 \text{ "Hg}$$

$$\rho_x = \frac{30.165 - (.36)(.4287)}{(.754)(531)} = .0749 \text{ lb}_m/\text{ft}^3$$

(4) Determine input horsepower.

$$HP_{in} = \frac{2400}{4000} \times 4.05 = 2.43 \text{ HP}$$

(5) Correct input horsepower for specified speed and density.

$$HP_{in} = 2.43 \times \left(\frac{2400}{2400}\right)^3 \times \frac{.0749}{.0749} = 2.43 \text{ HP}$$

(6) Correct P_s for specified speed and density.

$$P_s = 1.78 \times \left(\frac{2400}{2400}\right)^2 \times \frac{.0749}{.0749} = 1.78 \text{ "H}_2\text{O}$$

(7) Determine static efficiency, η_s using corrected values of Q, P_s and HP_{in}.

$$\eta_s = \frac{3710}{6356} \times \frac{1.78}{2.43} \times 100 = 42.8 \%$$

APPENDIX B

Tabulated results

Run	Q, CFM	P_s, in. H_2O	HP	η_s, %
1	3710	1.78	2.43	42.8
2	3190	2.60	2.44	53.4
3	2710	3.13	2.32	57.5
4	2450	3.38	2.29	56.9
5	2200	3.41	2.14	55.0

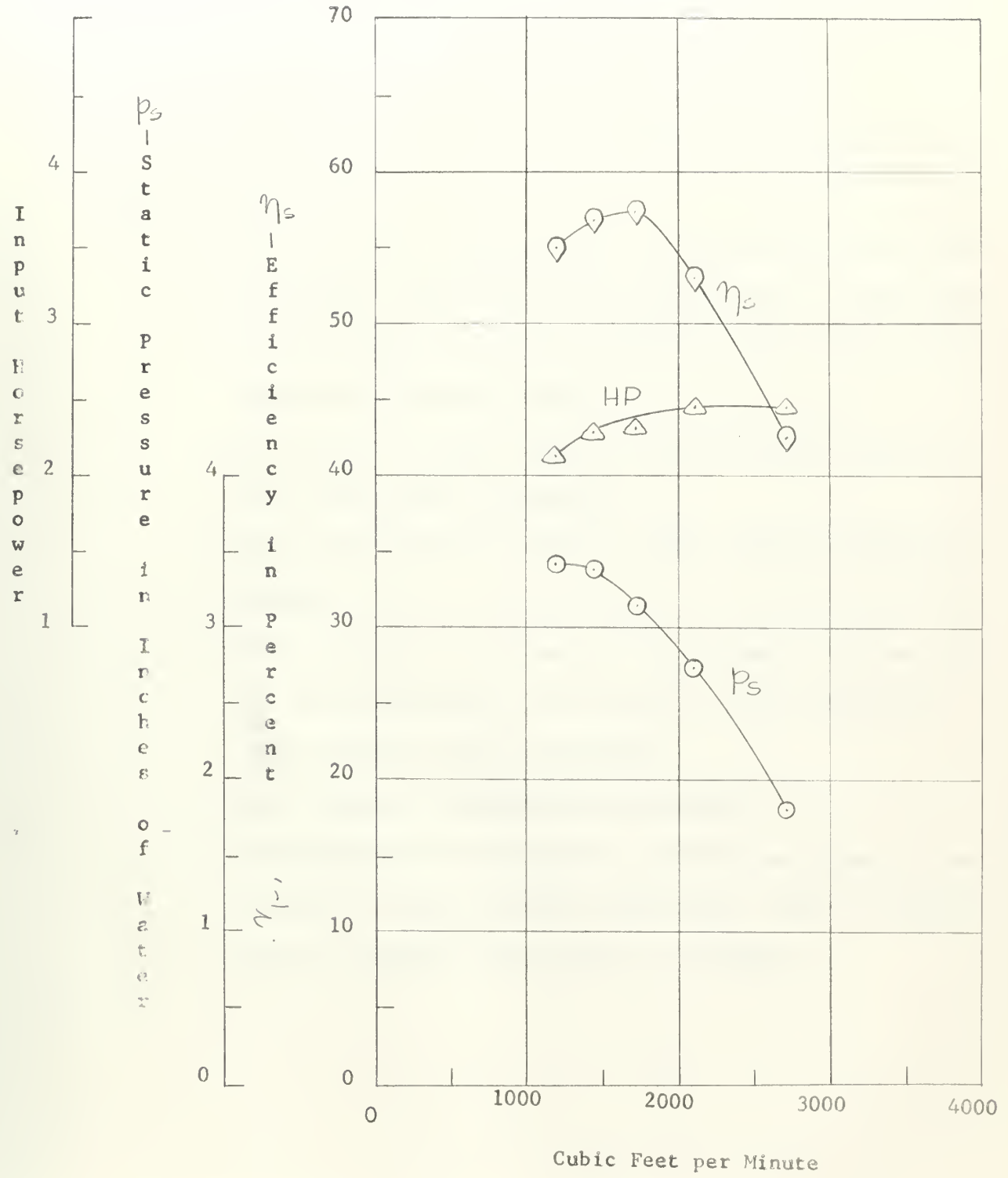

Figure 24. Results of sample calculations

APPENDIX C

1. Operating Instructions.

The following instructions are recommended for the operation of the fan-dynamometer set:

1. Remove covers from one or more flow metering nozzles, and ensure that throttling device is OPEN. Note: Throttling device closes with counter-clockwise motion of hand-crank - opens with clock-wise motion.
2. Close circuit breaker labeled "axial flow fan" located in wall power panel of laboratory.
3. Close line disconnect switch on speed variator power unit cabinet.
4. Make sure that all persons and loose objects are clear of the rotating machinery, and push MG set start button on speed variator power unit cabinet.
5. Push dynamometer RESET button on cabinet.
6. Push dynamometer START button on cabinet and bring unit up to speed by speed adjusting control knob. Note: Minimum speed is 500 RPM, maximum speed is 3000 RPM.

2. Safety Precautions.

The following safety precautions are recommended in connection with operation of the fan-dynamometer set.

(1) Never perform any work on any circuit, the fan, or the removable duct until all power is removed from the unit.

(2) Inspect fan-dynamometer set for foreign matter, such as nuts, bolts, tools, paper, etc. before starting.

(3) Do not wear loose neckties or other loose clothing or carry loose tools that may get caught in rotating parts.

(4) At least two persons should be present during all testing.

(5) Read and be familiar with contents of the instruction book.

```
SKIP LO          AMREADIN         001
SKIP LO          AMREADIN         003
SKIP LO          AMREADIN         007
SKIP LO          AMREADIN         009
SKIP LO          TPWTA            003
SKIP LO          TPWTB            003
SKIP LO          SUBB             003
SKIP LO          SUBB             005
SKIP LO          SUBBA            003
SKIP LO          SUBBA            005
SKIP LO          SUBBB            003
SKIP LO          SUBBC            019
SKIP LO          SUBBC            021
SKIP LO          SUBBD            007
SKIP LO          PARER            005
SKIP LO          PARER            007
SKIP LO          PARERA           001
SKIP LO          PARERA           003
SKIP LO          DUMPA            001
SKIP LO          DUMPA            007
SKIP LO          ERASE            003
SKIP LO          ERASE            005
SKIP LO          DUMPB            007
SKIP LO          DUMPB            009
SKIP LO          DUMPD            011
SKIP LO          DUMPD            013
SKIP LO          TPLDE            011
SKIP LO          TPLDE            013
SKIP LO          TPLDA            003
SKIP LO          TPLDA            005
SKIP LO          TPLDB            003
SKIP LO          TPLDB            005
SKIP LO          TPLDB            017
```

```
                                    REM     AUTO MONITOR ROUTINE OF 24 APRIL 1961
                                    ORG     5000
                                    REM     PREFACE T
05000   75 0 05014                  SLJ   0 C                       5000    MODIFIED WARD DUMP.
        50 0 00000                  FNI   0 0
05001   75 0 05024                  SLJ   0 AMSTART                 5001  AMSTART.
        50 0 00000                  FNI   0 0
05002   75 0 05362                  SLJ   0 B1                      5002  TSTLOAD
        50 0 00000                  FNI   0 0
05003   75 0 05004                  SLJ   0 AMREADIN                5003  AMREADIN
        50 0 00000                  FNI   0 0
05004   74 0 32031  AMREADIN        EXF   0 32031
        74 7 32000                  EXF   7 32000
05005   74 0 32005                  EXF   0 32005
        74 7 32000                  EXF   7 32000
05006   74 0 32031                  EXF   0 32031
        50 3 06000                  ENI   3 6000
05007   57 3 00003                  SIL   3 3
        74 7 32000                  EXF   7 32000
05010   74 3 05000                  EXF   3 5000
        74 7 32000                  EXF   7 32000
05011   74 7 32003                  EXF   7 32003
        76 0 05004                  SLS   0 AMREADIN
05012   74 7 32005                  EXF   7 32005
        76 0 05004                  SLS   0 AMREADIN
05013   76 0 05024                  SLS   0 AMSTART
        50 0 00000                  FNI   0 0
05014   56 1 05017  C               SIU   1 C+3                     MODIFIED WARDS DUMP
        57 4 05017                  SIL   4 C+3                     PLACE FIRST ADDRESS IN B BOX 1.
05015   12 0 05020                  LDA   0 C+4                     SECOND ADDRESS IN B BOX 4.
        20 0 70002                  STA   0 70002                   START AT 5000.
05016   75 0 00027                  SLJ   0 27                      FOR REPEAT ENTER NEW ADDRESSES RESTART
        50 0 00000                  FNI   0 0
05017   00 0 00000                    00  0 0
        00 0 00000                    00  0 0
05020   75 0 05021                  SLJ   0 C+5
        50 0 00000                  FNI   0 0
05021   12 0 05017                  LDA   0 C+3
        75 4 70002                  SLJ   4 70002
05022   50 1 00000                  FNI   1 0
        50 4 00000                  ENI   4 0
05023   75 0 05014                  SLS   0 C
        50 0 00000                  FNI   0 0
                                    REM     AMSTART L
05024   12 0 05030  AMSTART         LDA   0 AMSTARTA
        20 0 00007                  STA   0 7
05025   12 0 05031                  LDA   0 AMSTARTB
        74 0 00100                  EXF   0 100                     SELECTS INTERRUPT
05026   20 0 00000                  STA   0 0
        74 0 01000                  EXF   0 1000                    CLOCK SET AND STARTED
05027   75 0 05125                  SLJ   0 TPLKOUT+5
        50 0 00000                  ENI   0 0
05030   75 0 00000  AMSTARTA        SLJ   0 0
        75 0 05032                  SLJ   0 SUBA
05031   37 7 77777  AMSTARTB        OCT     3777777777777777
        77 7 77777
                                    REM     SUBA R
05032   20 0 05126  SUBA            STA   0 ATEMPST
        74 0 00070                  EXF   0 70
05033   12 0 05031                  LDA   0 AMSTARTB
        20 0 00000                  STA   0 0
05034   72 0 05412                  RAO   0 CLOCK
        75 1 05036                  SLJ   1 /+2
05035   75 0 05120                  SLJ   0 TPLKOUT
        50 0 00000                  FNI   0 0
05036   36 0 05135                  SSK   0 TPWTFLAG
        75 0 05072                  SLJ   0 TPWT
05037   74 7 32001                  EXF   7 32001                   EXIT ON NOT READING
        75 0 05057                  SLJ   0 TPWTENTR
05040   74 7 42001                  EXF   7 42001                   EXIT ON NOT WRITING
        75 0 05057                  SLJ   0 TPWTENTR
05041   57 6 05132                  SIL   6 I+2
        56 5 05132                  SIU   5 I+2
```